Model-Based Predictive Control of Window Shades

by

Brent Huchuk, **B.Sc., Engineering Physics**

Queen's University

A thesis submitted to the

Faculty of Graduate and Postdoctoral Affairs

in partial fulfillment of the requirements for the degree of

Master of Applied Science in Civil Engineering

Department of Civil and Environmental Engineering

Carleton University

Ottawa, Ontario

July, 2014

The undersigned hereby recommends to the

Faculty of Graduate and Postdoctoral Affairs

acceptance of the thesis

Model-Based Predictive Control of Window Shades

submitted by **Brent Huchuk**, **B.Sc., Engineering Physics**

Queen's University

in partial fulfillment of the requirements for the degree of

Master of Applied Science in Civil Engineering

Dr Liam O'Brien, Thesis Co-supervisor

Dr Cynthia A. Cruickshank, Thesis Co-supervisor

Dr Abass Braimah, Chair

Department of Civil and Environmental Engineering

Carleton University

July, 2014

Abstract

As architecture and engineering push the boundaries of what is possible with highly-glazed façades, the traditional approach of leaving shading control up to active occupants becomes a larger energy burden. Shades, if operated correctly, can provide substantial reductions both to the space conditioning loads of the building and its lighting use. Because of the delayed thermal response to solar gains, predictive controls are beneficial.

In this study, the framework for a transferable model-based predictive controlled shading solution is laid out. The analysis began with a numerical investigation into thermal model training using a Bayesian approach — namely the Ensemble Kalman Filter — for calibrating a low-order control model of the space. The trained model had its effectiveness demonstrated and was successfully utilized within the EnergyPlus environment to control the shades of single zone office and provide total electricity savings of 35% in a complete building automation system.

Later, these methodologies were adapted and utilized in a demonstrative setting built within a research facility to attempt and identify the challenges associated with the scaling of the approach. The results showed an environment which effectively managed occupant needs both visually and thermally and which ultimately was found to save energy in comparison the previously existing system in the building.

Acknowledgments

I first wish to acknowledge the efforts of both my supervisors, Dr. Liam O'Brien and Dr. Cynthia Cruickshank without whom none of this work would have made it this far. Their knowledge, skills and patience through this process were invaluable and I thank you for it.

I would like to acknowledge my colleagues within the Human Building Interaction Lab. Starting only with the dynamic duo of myself and Burak Gunay; we have grown to include many more individuals including Austin Selvig, Ryan Kuhne and Isis Bennet over the course of two years. I thank you all for you friendship and assistance when called upon. Additionally I wish to thank Jenny Chu, Jayson Bursill and Philippe Bisaillon for their critical assistance and knowledge at key times.

The support from the Natural Sciences and Engineering Research Council of Canada (NSERC), along with partnerships with Delta Controls and Regulvar provided the necessary resources to partake in this endeavour.

Finally, thank you to my family for all their support and encouragement through not just this process but everything leading up until this point.

Table of Contents

List of Tables

List of Figures

Chapter 1

Introduction

1.1 Background

Buildings account for over 50% of Canada's electrical energy use in both commercial and residential buildings for space heating/cooling and equipment and lighting demands [1]. The full breakdown of Canada's end use of energy in commercial and residential settings can be seen in Fig. 1 over a number of reported years. Any strategies to reduce the energy use for conditioning the space of a single building could then result in a huge opportunity at a nation-wide level if properly designed with transferability in mind.

Since the 1900s, the management of the indoor climates in buildings has been maintained through heating, ventilating and air conditioning (HVAC) systems or the actuation of window and window shading devices by the occupant(s). All of these strategies are controlled solely on the basis of instantaneous stimuli. For example, the heating or cooling equipment operates when the interior temperature exceeds or falls below a setpoint value. These systems are commissioned based on a set of standard setpoints which often do not account for the specific properties of the building. Even in those situations where attempts are made to utilize the building's

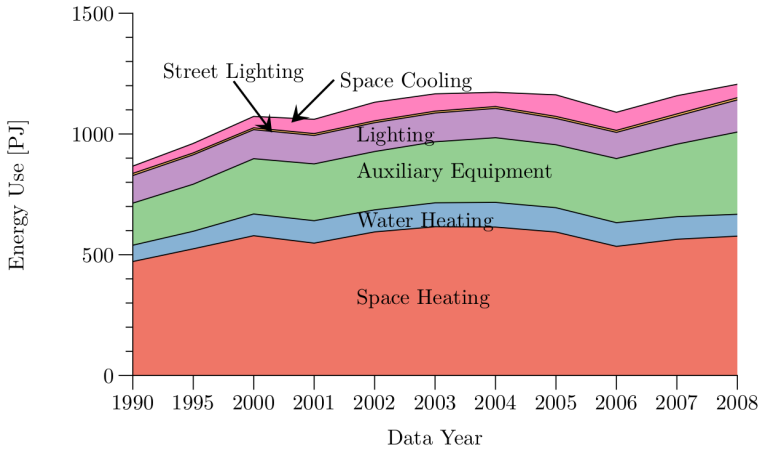

(a) Commercial

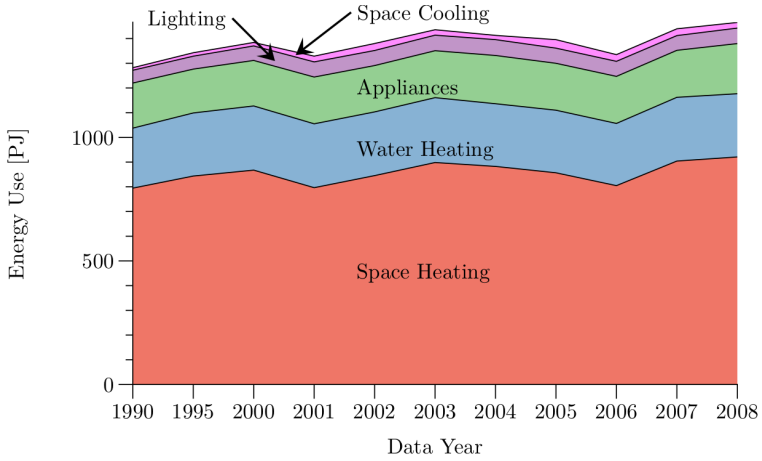

(b) Residential

Figure 1: Canadian energy end use data, data taken from NRCan [1].

physical characteristics, such as during optimal starts and stops, the commissioning is based on rules of thumb (e.g., calculations based on square footage) or estimates of the thermal capacitance. This approach relies on the experience of the technician and typically favours a conservative controls approach, which does not risk potential occupant discomfort.

At the same time as building controls are still designed very traditionally, there has been a growing increase in 'modern' building design which typically use highly-glazed façades. Whether motivated by aesthetic arguments or the potential occupant

benefits, the increasing technological innovations in glazed system construction (e.g., low-E or spectral selective coatings) have meant that it is common to find buildings that have substantial portions or entire façdes assembled of glazed materials. One of the most challenging issues with so much glazing is the controlling of the transmitted solar radiation (solar gains), on a scale never dealt with by traditional controllers, while managing visual comfort expectations. Compared to the more traditional air-based systems (i.e., entrainment or displacement ventilation), the effect of the high solar gains is thermally lagged. This effect is illustrated in Fig. 2. The peak outside temperature occurs after solar noon (the peak solar condition) while the peak room temperature occurs hours later then that. The room temperature profile is dependent on when a shading actuation occurs, say at either point A (peak solar) or B (peak outdoor temperature), and seasonally either point could be the ideal one depending on the current situation. In order to determine the effect of a control decision in the current hour then, the controller must know what the effects will be hours in advance.

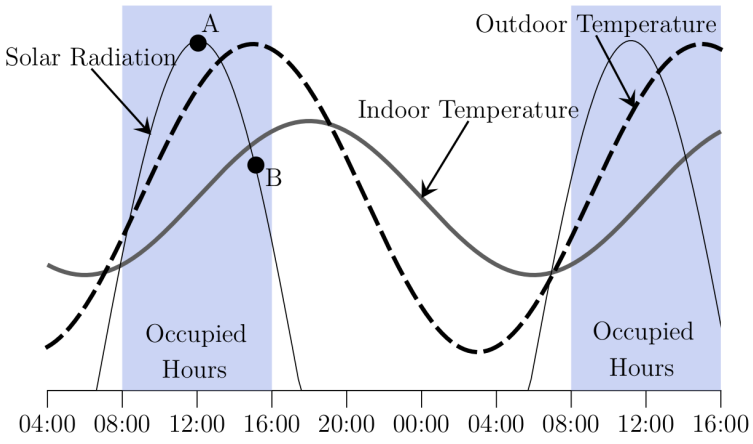

Figure 2: Thermal lag effects in buildings.

1.1.1 Managing Solar Gains

The solar gains of a building are usually managed by the proper selection of building construction materials or passive shading features developed in the design process. Even then, the control typically relies on the use of installed window shading devices. Moveable window shading devices (e.g., roller shades, venetian blinds, vertical blinds, etc.) are installed in most commercial buildings. Their control is often left to the discretion of the building occupants who are difficult to understand and rely upon for making ideal decisions. Their actuation movements are based on a number of visual and thermal stimuli that determine their level of comfort with the conditions. Researchers have attempted to summarize these conditions, including Kuhn *et al.* [2] and O'Brien *et al.* [3]. The summary of these stimuli from Kuhn *et al.* [2] is shown in Fig. 3. With so many stimuli resulting in control actions (including subjective metrics like glare), there is a high level of uncertainty in how occupants will actually utilize their shades. Making it more difficult still to rely on occupants, there is little incentive to reset these actions when the source of discomfort is removed [4–6]. This means shades are often left in a suboptimal position from an energy standpoint. The actuations are then very infrequent, responding more to changes in terms of weeks and months, and less responsive to short-term condition changes [3].

Since occupants are so inherently difficult to rely upon, the obvious progression in approach was the automation of building shades; which with ideal operation can be highly effective. Lee *et al.* [7] found automated shading could reduce total cooling and lighting energy along with the peak cooling loads. Tzempelikos and Athienitis [8] were better able to quantify savings and found that the optimal movement of shades was capable of reducing secondary energy use (lighting, heating and cooling) by 31%. These automated strategies are often set to look only at energy saving arguments so

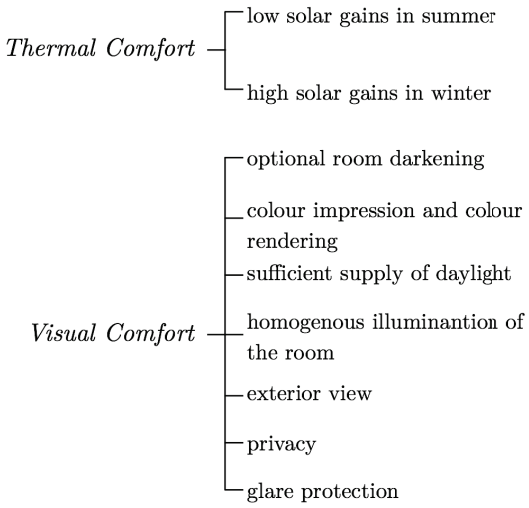

Figure 3: Comfort interactions of an occupant with window shades, adapted from Kuhn *et al.* [2].

the occupants begin to adapt and remove the benefits. In the work by Velds [9], automated venetian blinds were used to block direct sunlight from entering a workspace while a luminance sensing electric lighting system was designed to keep a workplace illuminance value of 500 lux (a common value selected based on investigation on visual comfort and glare, a topic expanded in Appendix A). The study with occupants found that they were frustrated by the lack of control over either system (about twice as unhappy for not having it with the lighting control). Reinhart and Voss [10] found that of 3005 automatic blind manipulations 45% were re-adjustments done manually as an override of the control algorithm of an automated blind system. In 88% of these, the occupants reversed the closing of the blinds. When automated shades are present, occupant mannerisms begin to change. Sutter *et al.* [11] found that users adjusted their blinds three times more often when the system was automated; most likely since it was now much easier to control. More extreme are the cases of well-documented adaptations to the automated system installed, such as was discovered by Konis [12] and shown in Fig. 4.

Figure 4: Example of personal space modification, reproduced with permission from Konis [12].

1.2 Problem Definition

While blinds have largely been ignored in their integration in predictive building systems their automation has been a curiosity to researchers and industry for decades [13]. Predictive control methodologies and heuristics are incredibly diverse with no one solution been proven better than the others yet — as can be seen by the lack of developed products or applications. Opposition by the building occupants has historically met attempts at blind automation. The goal then is to be able to develop a system that is easily implemented, effective at contributing savings but most importantly will not cause occupants to become hostile towards the system. The challenge in addressing and properly developing the system to answer all these questions exceeds the abilities of this investigation. Instead, the study will develop and answer the

questions, but will stop short of being able to get the long-term test results required to properly validate the methods.

1.3 Contribution of Research

Within the scope of current work:

1. the use of recursive parameter estimation for determining effective building thermal parameters was investigated;

2. a model-based predictive control strategy utilized in the EnergyPlus simulation environment for the thermal model's blind control was designed; and

3. an office-based test facility was commissioned in which automated blind controls were implemented and studied.

1.4 Organization of Research

The thesis is divided into the following chapters:

Chapter 2 discusses a survey of literature on the use of predictive controls in building applications and system calibrations of their associated control models. The concluding summary sets the foundation for this work.

Chapter 3 describes the numerical approaches devised. The baseline model developed as the basis of the simulation work is specified as is the formulation of both the model training methods and minimized cost functions.

Chapter 4 presents the results of the model training using all the developed methods. The chapter then presents and discusses a number of results from the

implementation of the MPC strategies including a number of design decisions made.

Chapter 5 outlines the steps taken to create a demonstration facility built on a newly commissioned building automation system. A brief series of results comparing the facility to a neighbouring office space are presented.

Chapter 6 discusses the feasibility of the MPC strategy for blind automation both in implementation and financial terms.

Chapter 7 provides the concluding remarks based on the simulation work and the demonstration facility. The chapter ends with a discussion on future work both as an extension of this study and into new research areas.

Appendices A through C present additional material which is supportive of the research presented, including MATLAB scripts, devised code for BACnet protocol and a report on visual comfort and glare.

Chapter 2

Literature Review

This chapter presents a review of the literature that is relevant to the present work and research. The review starts with an investigation of past studies and applications of predictive control in the building context using both complex and low-order control model methods. This is followed by an investigation on past research on the training approaches used in conjunction with these simplified models.

Many of these studies deal with buildings and their energy profiles. More details on these subjects and their subsequent calculations and histories can be found in other sources. Fundamental concepts of heat transfer and shading can also be found in sources such as Kuhn *et al.* [2]. A fundamental look at elements of visual comfort, an important theme of shade automation design, can be found in Appendix A.

2.1 Predictive Controls in Buildings

The predictive control of building systems is not a new idea but outside of academics, has not been widely applied [14]. The transition from predictive controls from more traditional heuristics, as is seen in much of the research, is usually not a hardware decision and most integration is only a software adjustment to already existing building

automation systems (BAS). Often when talking about the use of predictive control, model (or model-based) predictive controls (MPC) are discussed. MPC is an advanced technique for optimizing control by predicting system behaviour for a period of time and applying a cost function, which is minimized. In buildings, particularly with thermal storage technologies or a high thermal mass that looks to be utilized, control decision effects will not be felt for prolonged periods of time and as such a predictive methodology is required.

Predictive strategies in buildings are also an important topic in the development of demand responsive designs of building system and grid technologies. Demand response controls can benefit both the user and the utility through peak shaving and load shifting on the grid by the prediction of utility demands and prices [15]. The predictions are actuated at the building level across the grid to achieve the desired benefits. These demand response controls have been applied to numerous systems including HVAC and lighting and have looked both at short-term and long-term variables to the operation of buildings [16]. This high-level predictive strategy is already highly visible in the residential market, with such products as Ontario's peaksaver PLUS program.

2.1.1 Predictive Control Using Complex Models

In the mid-90s a simulation-based investigation on control strategies that could coordinate a dynamic building envelope with an electric lighting system for comfort and energy reduction was conducted by Lee and Selkowitz [17]. In this study, the researchers looked to develop and compare a predictive system and its performance with more traditional control strategies that were based on energy or lighting designs. Their predictive control strategy, as illustrated in Fig. 5, was designed to predict the

requirements of lighting and cooling and select the strategy that resulted in the minimum energy usage. In the implementation, this required the pre-calculation of the light and cooling energy balance for all positions and states of the systems (something computationally difficult even now 20 years later) at each timestep. As a result of their study, Lee and Selkowitz [17] found that regardless of the control strategy (reactive or predictive) any algorithms had to be designed to meet multiple performance criteria (i.e., electricity consumption, peak demand, cost, occupant preferences, etc.) and be able to resolve those contradictory situations between criteria. Further, and most importantly, any controls must be accommodating to occupant preferences (even at the cost of losses in savings) or risk becoming "sabotaged" by the occupant.

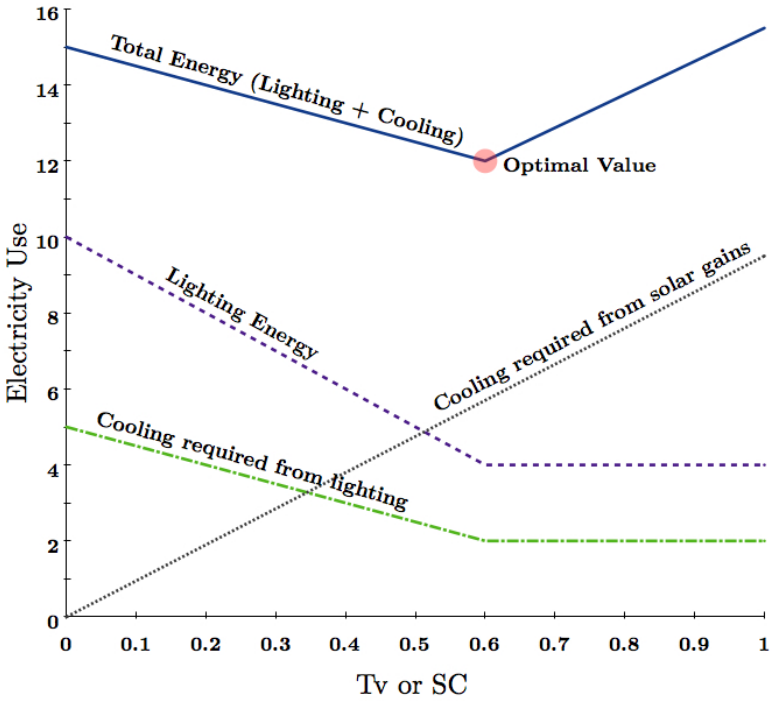

Figure 5: A conceptual diagram of cooling, lighting and summed electricity use as functions of shading coefficients (SC) or visible transmittance (Tv) for a hypothetical dynamic envelope and lighting system, adapted from Lee and Selkowtiz [17].

More recently May-Ostedorp *et al.* [14, 18] investigated the use of MPC for the operation of windows for commercial building use. The goal was to be able to extract rules offline from MPC results. Once these rules were extracted they could be easily implemented as the basis of the controls, as they are computationally more efficient than a dynamic model simulation. A proof-of-concept along with extensions into advanced data-mining techniques indicated the promise of this approach at controlling a building using an existent BAS while achieving the results of a more advanced MPC controller. The rule extraction method was found to reduce the potential electricity savings from the full MPC approach by 3% but computation used only one run as opposed to thousands of runs of a fully developed EnergyPlus model. The authors did acknowledge that significant work still remained to prove this approach in a real building system and required thorough investigation on the subject of non-ideal forecasts, a condition they had assumed.

Mahdavi and Pröglhöf [19] evaluated natural ventilation as a possible application for MPC. Part of that project looked at the complex effect that the opening of a window can have on an otherwise effective running HVAC system. Natural ventilation has the potential to keep occupants thermally comfortable while not relying on active thermal and cooling measures/systems but often is operated to counter the buildings active HVAC operation. Mahdavi [20] and Mahdavi *et al.* [21] investigated the use of prediction schemes for use in shading and daylighting controls. The approach relied on a self-updating model of the sky (based on calibrated digital photography) and judged shading position based on ranked preferences. Simulation results were promising enough that the system was incorporated into a system for testing [21]. Experimental testing in a full-scale facility found the controls to reliably create strategies that minimized the use of energy intensive building systems and effectively utilized natural light and ventilation.

Corbin *et al.* [22] sought to create an MPC strategy using a coupled optimizer between EnergyPlus and MATLAB. The researchers developed an online and offline methodology illustrated in Fig. 6. Though both are complex and reliant on a very robust system to be able to be implemented, only the relatively simpler offline variety was taken into testing. For determining the optimum process, a particle swarm optimization was implemented. Particle swarm optimizations can encounter complications as they are non-deterministic. This means convergence is not guaranteed or can be very time-consuming to achieve. Results on a standard building in which setbacks and thermostats were adjustable found savings of 5% over a baseline. In a building design in which more thermally active storage was available, savings were found to be possibly as high as 54%. Use of the EnergyPlus model was noted to be a hindrance to the process in its time requirement to run; something that was not as fatal a flaw in a system that was only actuating in hourly or multi-hour increments.

2.1.2 Predictive Control Using Reduced-Order Control Models

One of the largest projects on the investigation of MPC in a building application was the OptiControl project carried out in Switzerland by several academic institutions, government agencies and industrial partners [23]. The overall goal of the project was to "minimize the energy usage of buildings while maintaining or improving the occupant comfort and reducing peak electricity demand" by utilizing integrated room automation; which was the BAS at a building zone or room level. The integrated room automation was responsible for control over the the blinds, electric lighting, heating, cooling and ventilation. The project led to the development of advanced control algorithms for peak load reduction and climate control. Furthermore, the project

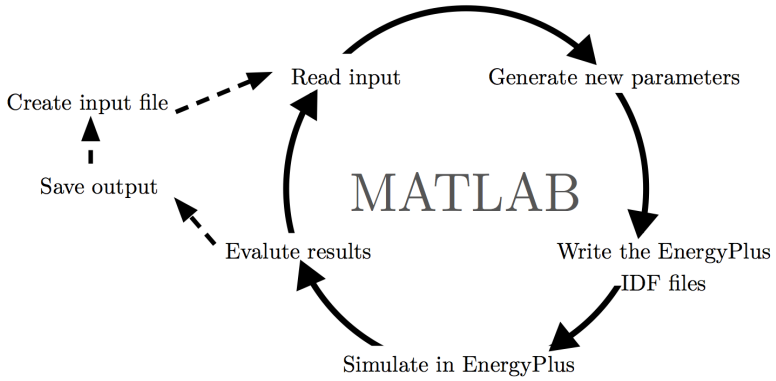

(a) Offline methodology

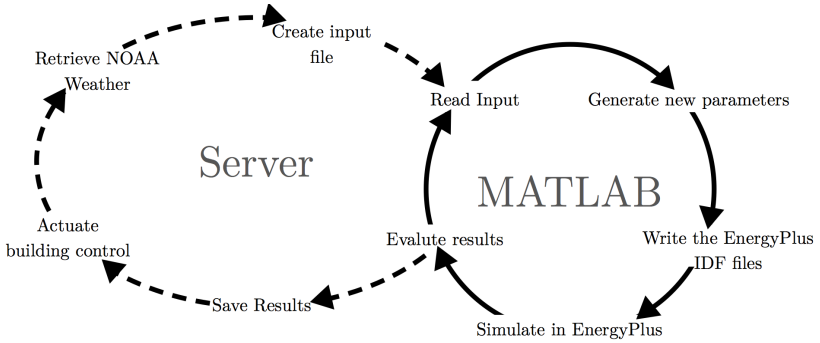

(b) Online methodology

Figure 6: MPC metholodologies adapted from Corbin *et al.* [22].

brought attention to the stochastic nature of dealing with a system with occupants and dynamic weather [24–27]. The predictions and controls were based on the complex resistance and capacitance (RC) model of the building and the subsystems shown in Fig. 7. Model parameters were treated as known characteristics about the system; something much more difficult to do in less fully understood and researched situations. Investigations showed the effectiveness of a two-level design (i.e., controls looking at long term and energy saving solutions and a second system which could be quick to react and ensure occupant comfort) [28, 29] along with the effectiveness of employing a predictive over rule-based control strategies, including shades [28].

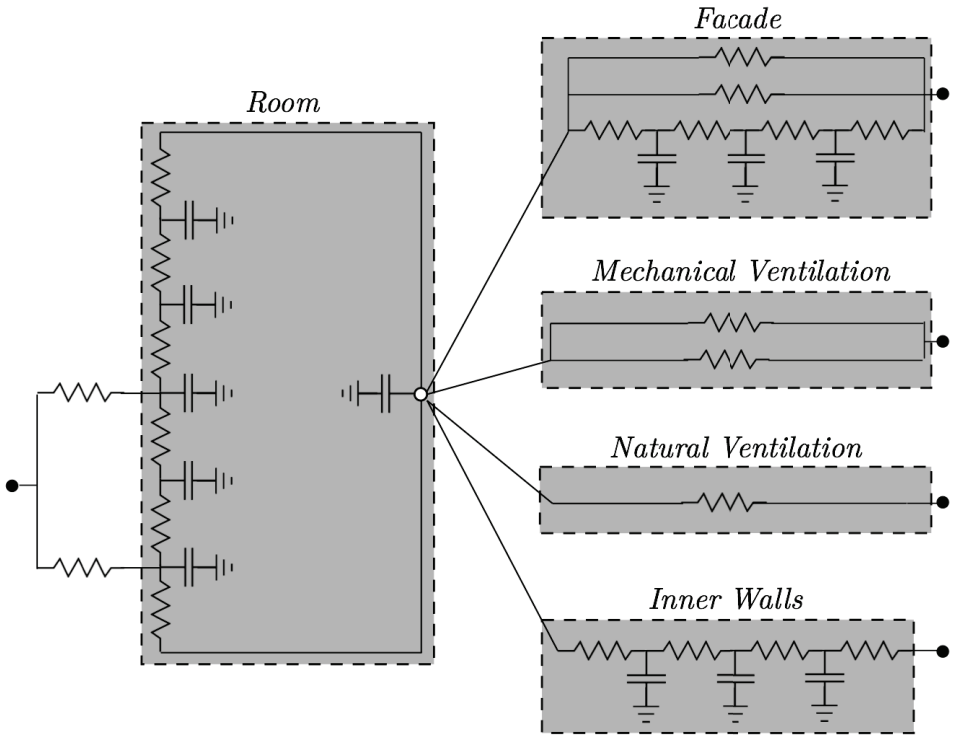

Figure 7: Thermal RC network showing all supported subsystems, adapted from Gyalistras *et al.* [23].

Ma *et al.* [30, 31] researched the use of MPC for the reduction of cooling through the predictive charging of a cooling system. The MPC was brought in to find the optimal control sequence to satisfy cooling loads while minimizing the electricity costs and improve the plant coefficient of performance (COP). The system relied on the predictive knowledge of building loads, forecasted through a reduced-order building network model using an RC building model, and weather forecasts to charge a large storage tank. The system was able to provide optimized scheduling and operation for the central plant at the University of California, Merced. In comparison between standard operation and the MPC managed systems, substantial reductions were achieved to the operation costs while moderate returns were made on the COP. For this reason, the authors felt price was to be a more beneficial metric for selling the idea to stakeholders than electricity use.

Passive solar buildings are designed to optimally utilize solar gains so space conditioning in both heating and cooling seasons does not rely on the use of mechanical or electrical means. Specific research has been conducted on predictive controls used in these passive solar buildings. Kummert *et al.* [32,33] and Kummert and André [34] were able to provide simulation and experimental results of RC model based MPC against more common controller practices. The model-based controller extended on more traditional energy and monetary cost functions developed by other researchers and added an associated cost of occupant comfort (based on the Predicted Percentage of Dissatisfied [35]). Looking only at the heating of the spaces, results found that a predictive system could provide saving and comfort improvements.

Radekci and Henecy [36] applied an MPC strategy as part of a completely integrated control scheme over a multi-zone building using a second-order RC model. A major, and unique, component of the control scheme was the use of an "Experiment Generator" that would apply modifications to the controls and operations at opportune times to better estimate parameters. Though only based on simple heuristics in this study, extensions on this topic were seen as a major research opportunity. Attention was drawn to potential issues with these inverse methods coming to physical impossibilities (such as negative values) and false convergence — both of which were addressed with an overall observation function (a role filled by human intervention) which helped prevent these issues. The MPC system's actuating of the HVAC resulted in a 7.5% reduction over the standard thermostat-based system.

2.2 System Calibration of the Low-Order Control Models

Many researchers, identifying the need and potential of predictive controls or optimal HVAC operation, have investigated the training of simplified building models. Techniques are as highly varied as the range of engineering applications in which inverse modelling techniques have historically been applied.

Chen and Athienitis [37], investigated the use of a recursive least-square approach for training a multi-parameter model which estimated a building's thermal behaviour. The authors attempted to model a test-room over a six-month period. In their approach they noted that the technique was limited by issues that could "significantly impact the quality of the recursive least-squares estimator". More concerning was the reported possibility of "unstable or physically meaningless estimated models" if excitations were non-perpetual or poorly captured. Even so, a high order polynomial was eventually trained that gave a 0.27°C average root mean square deviation over a 24 hour period between the modelled and actual behaviours. This high accuracy was possible with very well processed data in which high-frequency white noise was removed from all the model inputs. This is much more feasible in the direct solar gain-test room which was monitored using well calibrated devices then a more standard building situation.

Dewson *et al.* [38] attempted to use a least-square method to solve a simplified building model constructed of five building parameters. The results indicated that under very well controlled situations the least-square approach was capable of producing a model capable of having an error of only 1°C, however the model was plagued with under-prediction of peak indoor temperatures. Further the authors noted general issues in: (1) non-uniqueness of solutions, (2) dependence on the initial conditions on

the avoidance of local minima and (3) a large variation in parameter values between subsequent training runs. A major conclusion drawn was the need for parameters to adapt in these simplified models when being used as the basis for a building energy management (BEM) system; a major advantage of more recursive techniques.

Braun and Chaturvedi [39] looked to calibrate models capable of predicting transient cooling and heating requirements. Their approach relied on the use of accurate initial estimates with prescribed bounds for the parameters in their RC model. Optimal values were found by utilizing a "global direct search algorithm" on the transfer function version of the equations. These estimates were augmented with a nonlinear regression algorithm. This stylisation of a *hybrid* approach can be very powerful but direct and global search algorithms can be very computationally demanding, especially with poor initial guesses. Even so, the authors managed to train a model using only two weeks of field data to calibrate a model capable of predicting cooling loads within about a 9% error.

Fux *et al.* [40] proposed a Bayesian approach to the online modelling of a first-order (as defined in Sec. 3.3.1) RC model using the extended Kalman Filter (EKF). An investigation into the training of various orders of simplified models had resulted in similar issues to those encountered by other researchers attempting to train a model. This motivated the progression to a self-adaptive approach achieved using the EKF; particularly in systems with non-quantified perturbations. Results of the study showed the EKF fulfilled its design requirements but results were a 'best-case scenario' since the study was based on a very unique passive house located in the Swiss Alps with low occupation. The researchers attempted to estimate the disturbances (occupant heat gains) simultaneously with the states. The authors however assumed that these disturbances were governed by a periodicity on both daily and monthly scales. This is known to be an oversimplification of the system as these patterns tend

to be much more stochastic. As such, during the training, the disturbance value can be artificially inflated leading to difficulty in the training of the R and C value.

Radecki and Henecy [41] utilized another Bayesian approach with the unscented Kalman Filter (UKF). Similar to Fux *et al.*, [40] the author's trained a low-order RC model for use as part of a control system for a building. As part of the investigation, the author's compared results of the UKF to an EKF and found the UKF to be both easier to implement (as it does not require the calculation of a Jacobian) and on repeated runs was much less susceptible to divergence during parameter estimation. Further in line with Fux *et al.* [40], the authors also sought to predict disturbances but only after the R and C values were nearly estimated. The authors once again assumed that these disturbances were highly standardized over a 24 hour period and cyclic. The model predictions were highly dependent on these disturbance models in order to achieve reasonable results with the baseline model.

Candanedo and Athienitis [42] explored the use of simplified linear transfer models for the development of control strategies in solar homes. Solar homes provide a unique testing opportunity because of their usually increased thermal mass, meaning thermal changes are much slower to react, along with their usual inclusion of motorized blinds or advanced control systems. The methodology used MATLAB's System Identification Toolbox to determine a transfer function for the building's thermal response. The model was applied to the control by finding a setpoint sequence that minimized a cost function over a control horizon (the MPC process). Though effective both as a modelling technique and control basis, the approach required a high-order (in this case a system with three capacitances was selected) Laplace Transform function to be calculated. Without the required computational capacity this poses many feasibility issues.

Candanedo *et al.* [43] worked on developing a control-oriented simplified modelling strategy for MPC. A third-order thermal network had its state space representation calibrated using the MATLAB Optimization toolbox. As a demonstration of the concept, the measured data was created using an EnergyPlus simulation of a five-zone office building. Training data was limited to only a few parameters including: operative temperature, solar gains, internal gains, exterior temperature and the heating/cooling powers. The demonstrated process showed promise but the authors acknowledged questions in the scalability of many of the process particulars. Such things as the model order were noted as being highly dependent on the situation to which the method was being applied. The potential value in taking the process offline and based on general rules were mentioned, but not explored.

2.3 Summary

Several different approaches for the implementation of MPC methods within the the building context were reviewed. A number of methods were found to be effective in their applications but all were met with challenges and lacked a transferability in their techniques. For that reason many of the elements of the MPC control structure will no be extended from the past investigations and will look more to inspire a new control strategy.

Moving forward, the control architecture will utilize an RC model similar to the studies in Sec. 2.1.2. These models had similar benefits to the full models without many of the challenges. A recursive methodology for parameter estimation based on the works of Radecki and Henecy [41] and Fux *et al.*, [40] will be applied but alternative versions of the approach that has unique characteristics will be considered.

Chapter 3

Methodology

3.1 Introduction

In order to accomplish the problem designed, a certain methodology was followed. Initially it was determined simulation would be the appropriate basis of design. As such a baseline model was designed as a comparison of savings between predictive and traditional heuristic-based approaches. Following that the predictive methods were designed. Identifying the need for an accurate model that could be easily implemented an investigation into different model sizes and the effectiveness of a proven technique from other applications was conducted. Based on these findings, an MPC control was assembled into EnergyPlus and utilized by the simulation as a control method. Lastly these controls were adjusted to find optimal control strategies and to include different optimization techniques as well as consider the comfort of occupants in the decision process.

3.2 Baseline Modelling

With no building at the disposal of the research that had a complete enough historical data set of all key variables, a simulation approach was initially required. As such, a baseline thermal model that could be actively measured and adjusted by the researchers was developed. Of the three main building performance simulation (BPS) tools actively used in research (EnergyPlus, ESP-r and TRANSYS), EnergyPlus was selected as the tool of choice for this research. It is one of the most accepted and widely used BPS tool, with detailed documentation available elsewhere (such as Lawrence Berkeley National Laboratory [44]). EnergyPlus has the added benefit of being very well equipped with auxiliary programs and support, including well-developed coupling with OpenStudio and SketchUp. These capabilities significantly increase functionality without an increase in required training or experience.

The geometry of a single rectangular thermal zone, hereafter referred to as the *shoebox model*, was designed in SketchUp. The office was modelled with 8 m^2 of exterior, south-facing exterior window and 7 m^2 of exterior wall area. The concrete floor slab was set to have an area of 25 m^2 and a thickness of 0.15 m. This basic geometry is captured in Fig. 8.

Further specifications were made within EnergyPlus to be able to thermally model the zone. The interior walls were set as adiabatic; an assumption based on the assumed symmetric boundaries with the rest of the building. Windows were modelled using a simple glazing system, and were specified to have a solar heat gain coefficient (SHGC) of 0.6 and a corresponding U-factor of 2 $W \cdot m^{-2} \cdot K^{-1}$. Infiltration and ventilation were set to have a combined air change rate of 0.5 air changes per hour (ACH). Heating and cooling demands were met using an ideal loads air system using nighttime setback thermostat settings. The ideal loads system was not connected to a

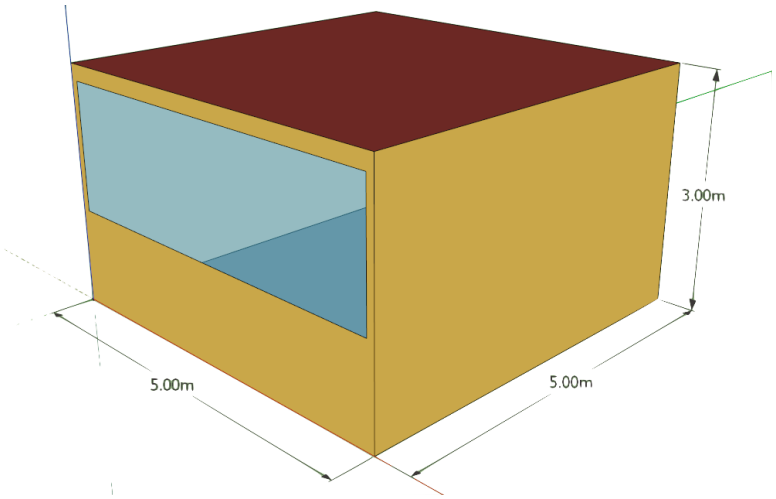

Figure 8: Isometric view of the *shoebox model* generated in SketchUp.

central air system and instead was modelled as a variable air volume (VAV) terminal unit, which provided the required supply temperature and humidity to meet the loads of the space. For cooling, temperature setpoints were set at 24°C and 28°C for occupied and unoccupied periods respectively. For heating, setpoints were set at 21°C and 16°C for occupied and unoccupied periods respectively. Occupancy was assumed to be a fixed 9:00 am-5:00 pm weekday routine for a single occupant who provided an internal heat gain of 100 W (with a sensible fraction of 0.6). Other internal gains were included for lighting at a power density of 10 $\mathrm{W} \cdot \mathrm{m}^{-2}$ and miscellaneous equipment at 5.4 $\mathrm{W} \cdot \mathrm{m}^{-2}$ [45]. Lights were automated in a strictly binary matter (i.e., on or off), and were tasked with providing 500 lux at the workplane defined 0.8 m above the floor in the centre of the room. All simulations were modelled in Ottawa, Ontario, an ASHRAE Zone 6 climate.

3.2.1 Baseline Building Automation

In order to compare any developed control strategies, a baseline performance model was needed. Based on the same building model as the predictive strategies, a situation

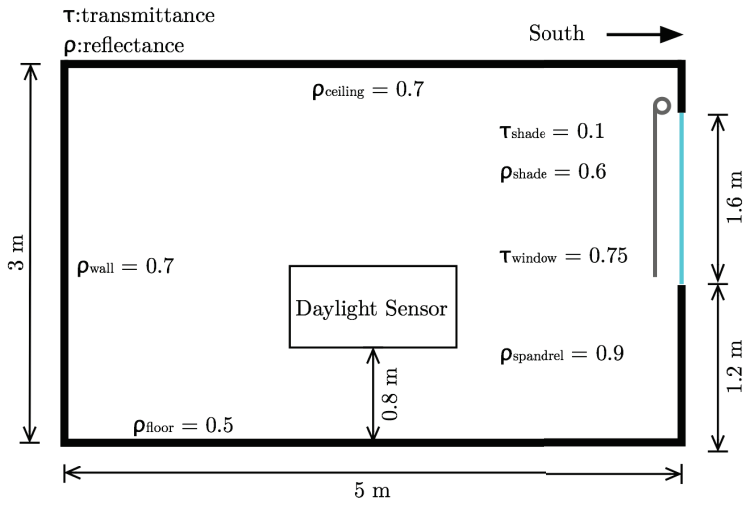

Figure 9: Elevation view of office space modelled in EnergyPlus and OpenStudio.

in which a building owner had installed automated shades for the workspace was created. The shades were designed to operate similar to the manual controls observed by Newsham [46], and later implemented by Reinhart [47] as automated shading in his Lightswitch-2002 algorithm. The control scheme is illustrated in Fig. 10. Of particular interest is the general level of inactivity in terms of blind movement occurring. The opening of the shades occurs upon their entry in the morning. In this strategy, the blinds are used as a visual control and are closed either when beam radiation is striking the occupant or else when the intensity outside exceed the 233 $\mathrm{W} \cdot \mathrm{m}^{-2}$. The lights in the zone were considered to be to be activated when the occupants arrived and turned off upon their departure for the evening with no opportunity for dimming; a fairly standard occurrence [46, 47].

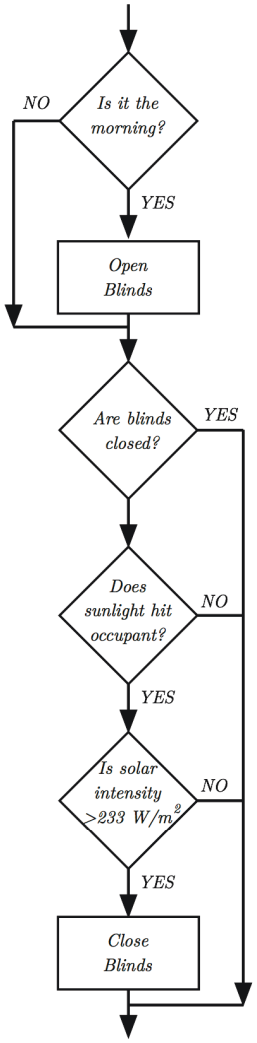

Figure 10: A model representing the action of an occupant, adapted from Newsham [46].

3.3 Controller Methods

The controller methods are the fundamental topics upon which implemented control were designed. Included are the summary of training methods and structure of the MPC approach.

3.3.1 Lumped Capacitance Model

The implementation of controls using a fully calibrated thermal model, such as that described in Sec. 3.2, has been attempted by others [14,18,22]. An approach similar to that was designed earlier using a coupled system with MATLAB [48], which eventually became the basis for predictive controls on the Team Ontario Solar Decathlon project. It is difficult to imagine such a model be created and maintained for each building that exists even as more buildings are being modelled then ever. Adding to the complicating factors, as the buildings get larger so do the models. These larger models become more difficult to incorporate into control decisions and keep up-to-date with changes in the buildings performance. For these reasons, a smaller model was deemed to be necessary. Moreover if it could be trained, the need for detailed building and material knowledge would be removed. Lumped capacitance models, similar to those found in research already for building controls [39–41] seemed ideal.

Lumped capacitance models can be formed either as white box or gray box models. White box models are models in which the underlying physics are fully understood and parameters known, represented as the ability to see the gears within the box in Fig. 11(a). Black box models are defined as a system where nothing is known about the system; only the input and outputs are known, as illustrated as in Fig. 11(b) in which nothing inside the box can be 'seen'. The gray box models fall in-between these two classifications. In it, the governing relationship is partially understood (or a simplified relationship is) and the parameters, often effective values, can somehow be determined. As an example, EnergyPlus models would be classified as a white box model. The emphasis here shall be placed on the successful implementation of a lumped capacitance gray box model.

The models are based off of electrical circuit analogy: R represents a thermal

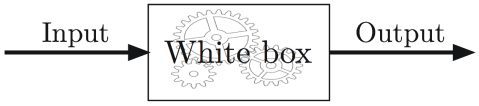

(a) White box

(b) Black box

Figure 11: Model classifications.

resistance (how energy flow is reduced) and C represents a thermal capacitance (how the energy is stored or released). The nodes connected between the electrical components are points where voltage would be measured, but here represent a temperature. The model order is equal to the number of capacitances within the circuit and can be solved using differential equations or finite equations. A graphical representation of thermal models of different orders can be seen in Fig. 12.

For this investigation the order of the model was limited to only two options, a first and second-order. Some researchers have noted the ability of first-order models to be acceptable for the needs of MPC control strategies [40, 41], particularly in shorter periods of prediction or smaller zones. Meanwhile many researchers have found that models using multiple capacitances better performed then a first-order model [49–52]. For controls applications, the simpler the model the easier it is to introduce into the existing BAS of a building.

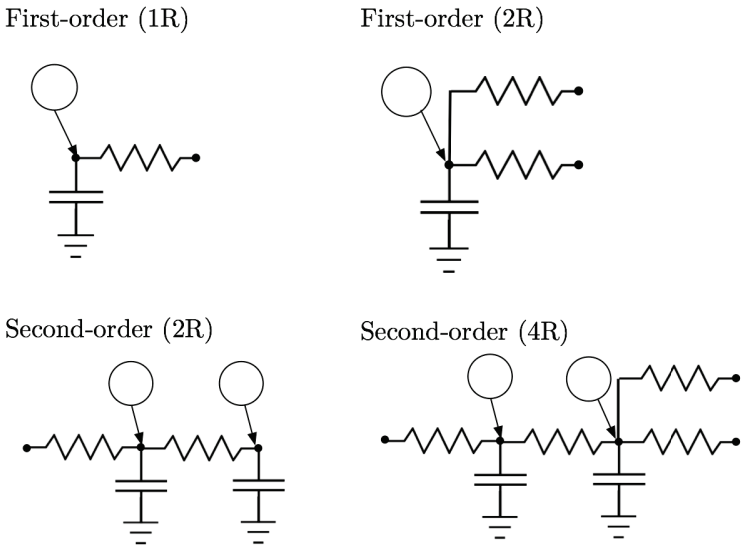

Figure 12: RC representations of various ordered models.

First-Order Building Model

In a first-order model, a single R and a single C are used. A schematic of this can be found in Fig. 13. In this case the R value represents the effective resistance between the ambient temperature (T_{amb}) and the indoor air temperature (T_{air}) while the C term represents the effective capacitance of the thermal zone.

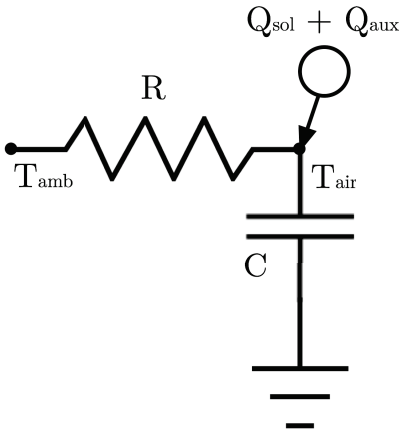

Figure 13: First-order schematic of a building model.

The physics of the space are governed by the laws of heat transfer that can be solved using the explicit finite difference equation expressed as Eqn. 1. Here the subscript k represents the timestep, while j is an index for the current node and i is an index for all connected nodes to the current node (j). The explicit finite difference method, is a numerical alternative to the analytical solution of the governing partial differential equations (PDE). By linearising the Taylor series expansion of the PDE's and assuming the parameters are time-independent at each instant. The space can be discretized into nodes, each with its own independent set of equations that rely only on the present values. Though the finite difference method assumes linearity and invariability which contributes to its difficulty in validation in comparison to analytical methods. Its unconditional stability and realistic testing however still make it a preferred methodology [53].

For this system, the equation can be expressed more specifically as shown in Eqn. 2. The indoor air temp (T_{air}) and outdoor temperature (T_{amb}) along with the energy rates from the HVAC and solar gains are assumed to be measurable and accessible to the building control system (e.g., via the building automation system or a local weather station). The R represents the effective thermal resistance of the interior space to the ambient conditions while the C represents the ability of the space to store and release the energy. The Q_{sol} term represents the solar gains incident on the exterior surface of the room and Q_{aux} represents the added or removed energy in the zone (e.g., internal load gains, HVAC loads, etc.).

The first-order model is not without its limitations and would be ill-suited for certain applications. For example, modelling a space of with high thermal mass could lead to inaccurate results. Since the first-order model assumes that all energy is directly transferred to the the air node and does not account for components which are radiated to the thermal capacitance there are instantaneous temperature movements

that exceed the real system. In high thermal mass buildings this splitting of energy results in a secondary release of energy, which is slower and has a significant effect.

$$\mathrm{T_{j,\,k+1}} = \frac{\Delta t}{\mathrm{C_i}} \left[\mathrm{Q} + \sum_{\mathrm{j}} \frac{\mathrm{T_{j,\,k}} - \mathrm{T_{i,\,k}}}{\mathrm{R_{i,j}}} \right] + \mathrm{T_{j,\,k}} \tag{1}$$

$$\mathrm{T_{air,\,k+1}} = \frac{\Delta t}{\mathrm{C}} \left[\mathrm{Q_{aux}} + \mathrm{Q_{sol}} + \frac{\mathrm{T_{air,\,k}} - \mathrm{T_{amb,\,k}}}{\mathrm{R}} \right] + \mathrm{T_{air,\,k}} \tag{2}$$

Second-Order Building Model

The second-order model breaks the system into more nodes, each which has its own set of equations. With its increased number of nodes and finer resolution (compared to the first-order model) the second-order model should be better able to capture the thermal response of the zone. One of the major issues it addresses is the splitting of energy gains or removals from only occurring at the air node. An illustrating representation of the model can be found in Fig. 14.

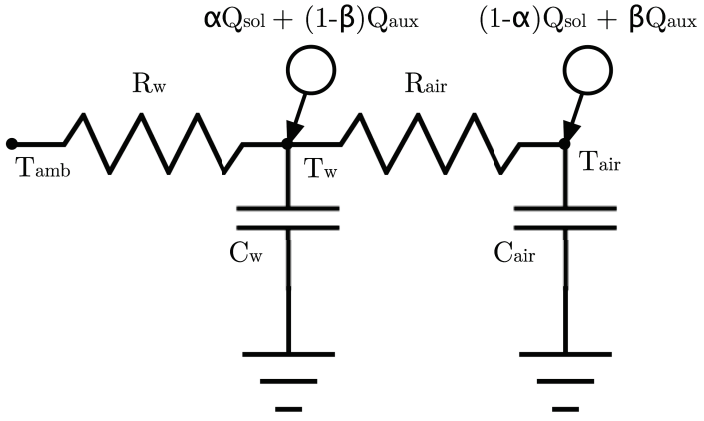

Figure 14: Second-order building model schematic.

The lumped resistance term, R_{air}, represents the effective thermal resistance between the walls and the interior air. The lumped capacitance term, C_{air}, represents the combined thermal mass of the air and contents of the room. The term R_w represents the thermal resistance between the zone and the exterior environments while C_w is the lumped capacitance of the zone construction. The Q's represent the same energy rates as before in the first-order models (Sec. 3.3.1). The α and β are fractions to represent the fraction of the loads that are released at the air versus surface node.

The general explicit finite difference equation (Eqn. 1) is defined for the two nodes represented in this model as Eqn. 3 and Eqn. 4. In order to determine the indoor air temperature (T_{air}) both equations are required to be solved at each timestep and represent two states either to be measured or predicted. The system is assumed to have similar access to information that the first-order model was given.

$$T_{air,\,k+1} = \frac{\Delta t}{C_{air}} \left[(1-\alpha) Q_{sol} + \beta Q_{aux} + \frac{T_{w,\,k} - T_{air,\,k}}{R_{air}} \right] + T_{air,\,k} \tag{3}$$

$$T_{w,\,k+1} = \frac{\Delta t}{C_{w}} \left[\alpha Q_{sol} + (1-\beta) Q_{aux} + \frac{T_{amb,\,k} - T_{w,\,k}}{R_{w}} + \frac{T_{air,\,k} - T_{w,\,k}}{R_{air}} \right] + T_{w,\,k} \tag{4}$$

3.3.2 Parameter Estimation

For use as a building model, the effective value of the C's and R's (in either the first or second-order models) must be determined based on the thermal zone(s) of study. These values are unique for each set of constructions [39, 40] and need to reflect the 'as-built' situation. To successfully calibrate these parameters manually would be tedious and nearly impossible, so inverse modelling methods are employed to

automate and expedite the process in a reliable manner. A number of past approaches were discussed in Sec. 2.2, all of which had their own unique set of shortcomings. More traditional methods such as recursive least-squares could be implemented when the state measurements are assumed perfectly known and non-corrupted by noise. For the first-order model this would have been acceptable as the only state (T_{air}) is measured. The second-order model would not be valid because of the unmeasured second state (T_w). A statistical-based method would be better suited in this case as it does not require the same deterministic conditions. Similar to Radecki and Henecy [41] and Fux *et al.* [40] a Bayesian approach was developed — the EnKF — as its inclusion of random sampling was felt to give a more robust solution then other's attempts.

3.3.3 The Ensemble Kalman Filter

The Ensemble Kalman Filter, is a recursive parameter and state estimation algorithm meaning it will continually update and improve estimates of both. Previously it has been used in various engineering applications and in climate modelling [54]. The EnKF carries an *ensemble* of values (based on random sampling based on probabilities) for its prediction and updating — similar to a particle filter — but it is much more efficient to operate. Compared to other Kalman filtering techniques, such as the UKF and the EKF, the EnKF better handles closure issues in the covariance (the variance of multiple items simultaneously) calculations [55] and does not require the calculation of the Jacobian (which requires a function to be derived and the derivatives taken) to deal with non-linearity (like the EKF) or deterministic sampling (like the UKF). Further the EnKF avoids the problem of maintaining the covariance of the EKF and UKF resulting in unreliable and unstable variable estimates when the modelled system is highly non-linear; as it is in the building heat transfer problems and during joint state and parameter estimation [56, 57].

The EnKF's origins come from the standard Kalman Filter (KF) [58] and so any derivation is obligated to begin there. In the most basic terms, the KF creates a weighted relation between an incoming observation and a prior estimation and iterates this process as new information becomes available. More formally, the KF starts with a state vector $\mathbf{x}$ (which is n-dimensional) which contains the estimates of the states and parameters (i.e., the R's, C's and temperatures). It is assumed to have a Gaussian probability distribution so it is definable as a mean (μ) and a covariance (Q). The variable selection and derivation here follows closely to the work of Mandel [59]. The probability density function (pdf) of this state vector, when assumed Gaussian, can be expressed such as in Eqn. 5. This pdf is referred to as the *prior*.

$$p(\mathbf{x}) \propto \exp\left(-\frac{1}{2}\left(\mathbf{x}-\mu\right)^{\mathrm{T}} Q^{-1}\left(\mathbf{x}-\mu\right)\right) \tag{5}$$

New data ($\mathbf{d}$) is collected on the system, in this case the new air temperature measurement in the space. The data has a known Gaussian pdf, which has a covariance of R and a mean of $H\mathbf{x}$ (where H is an observational matrix and relates the measurement to the forecasted state). The *prior* and the measurements are blended to determine the *data likelihood* that captures the pdf of the data $\mathbf{d}$ being collected based on the system state $\mathbf{x}$. This *data likelihood* is expressed as Eqn. 6. In this application it answers the question: "What is the probability of this air temperature measurement considering the current environmental conditions and latest R and C estimates?"

$$p(\mathbf{d}|\mathbf{x}) \propto \exp\left(-\frac{1}{2}\left(\mathbf{d}-H\mathbf{x}\right)^{\mathrm{T}} R^{-1}\left(\mathbf{d}-H\mathbf{x}\right)\right) \tag{6}$$

When the *prior* and *data likelihood* are combined using Bayes Theorem, the produce a new pdf referred to as the *posterior* which can be expressed as Eqn. 7. This

posterior is the new 'best estimate' of the what the parameter values are.

$$p(\mathbf{x}|\mathbf{d}) \propto p(\mathbf{d}|\mathbf{x})p(\mathbf{x}) \tag{7}$$

Once the measurement $\mathbf{d}$ has been utilized it has become set as a value so the state $\mathbf{d}|\mathbf{x}$ is defined as $\hat{x}$. Since both the *prior* and *data likelihood* were Gaussian initially, their resulting pdf will also be Gaussian. This new *posterior pdf* will be of the form of Eqn. 8, in which $\hat{\mu}$ and $\hat{Q}$ are new *posterior* means and covariance matrices defined in Eqn. 9 and Eqn. 10 respectively.

$$p(\hat{x}) \propto \exp\left(-\frac{1}{2}\left(\hat{x}-\hat{\mu}\right)^{\mathrm{T}} P^{-1}\left(\hat{x}-\hat{\mu}\right)\right) \tag{8}$$

$$\hat{\mu} = \mu + K\left(\mathbf{d} - H\mu\right) \tag{9}$$

$$\hat{Q} = \left(I - KH\right)Q \tag{10}$$

Both of $\hat{\mu}$ and $\hat{Q}$ rely on the the K matrix, which is officially referred to as the *Kalman Gain Matrix*. This matrix takes the form of Eqn. 11, and is what adjusts the estimates of R and C to their updated value.

$$K = QH^{\mathrm{T}}\left(HQH^{\mathrm{T}} + R\right)^{-1} \tag{11}$$

As the values evolve through this repeated process the associated errors diminish but never disappear. Ultimately it is impossible to get a value with no error associated as the measurement values (of the temperature) are always assumed to have been biased by an error.

The EnKF was developed by Evensen [55] originally to address computational challenges regarding the difficulty in maintaining these covariance matrices, particularly in large data sets or in situations where the state parameters are not independent. The EnKF is a Monte Carlo approximation to the standard Kalman Filter. Instead of maintaining the covariance matrix for the pdf of $\mathbf{x}$, it is maintained in an *ensemble* which is a representative sample X (defined in Eqn. 12).

$$X = [\mathbf{x}_1, \mathbf{x}_2, ..., \mathbf{x}_N] = [\mathbf{x}_i] \tag{12}$$

This *ensemble* is an $n \times N$ matrix, which has N columns representing the number of samples taken randomly from the estimates of the state and parameter's *prior* distribution. For this reason the matrix X is referred to as the *prior matrix*. The data ($\mathbf{d}$) is implemented in an $m \times N$ matrix D (Eqn. 13), where m is the number of measurement points.

$$D = [\mathbf{d}_1, \mathbf{d}_2, ..., \mathbf{d}_N] = [\mathbf{d}_i] \tag{13}$$

A *posterior* distribution from the samples can be achieved from the solving of the Eqn. 14.

$$\hat{X} = X + K\left(D - HX\right) \tag{14}$$

The Kalman gain is computed using the same general form as Eqn. 11 except the state covariance matrix (Q) is now replaced with the sample covariance (C) and appears like that in Eqn. 15

$$K = CH^{\mathrm{T}}\left(HCH^{\mathrm{T}} + R\right)^{-1} \tag{15}$$

The general concept in its application is shown as in Fig. 15. The update step begins with processing of an observation that is compared with the predictions using the calculated *Kalman Gain*. Finally the updating step is completed when state and covariance predictions are improved using the *Kalman Gain*. In this situation, the states estimated are the temperature of the nodes, while the parameters are the effective material properties of thermal resistance and capacitance. A more complete and thorough explanation of the EnKF and its methods can be found elsewhere, such as Evensen [60].

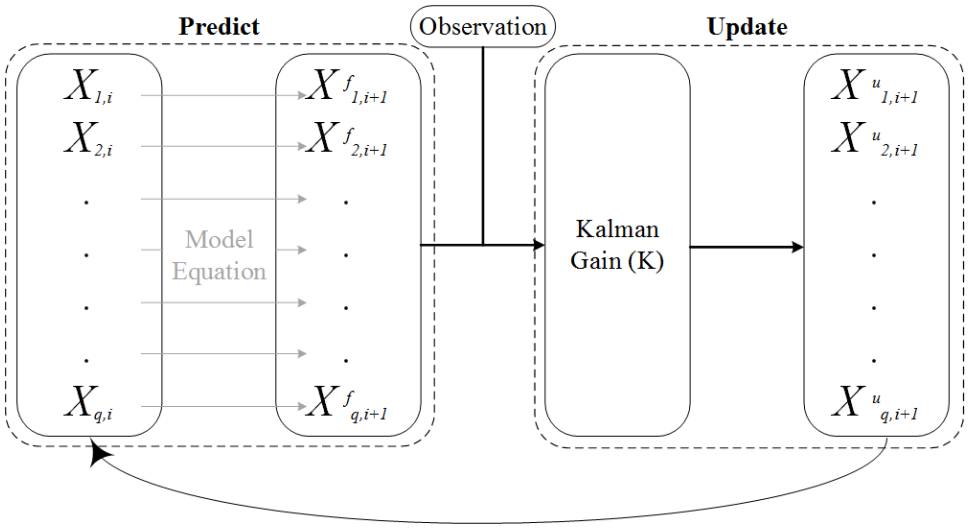

Figure 15: Schematic of the EnKF process.

3.3.4 Global Optimization

Just as the EnKF attempted to find the optimal values of R and C to fit the model as new data was introduced, other methods exist to provide the same functionality. To provide a further comparison to the R and C values a global search approach was attempted for the first-order model only. Similar in design to the training conducted by Kramer [61], the method relied heavily on standard MATLAB functions to find

the minimum error based on adjusted R and C values. This MATLAB reliance and computational power requirement makes it ill-suited for any widespread application (e.g., in a controller). Starting with an initial estimate of values, the response of the first-order model is predicted over a time window. The minimization function is calculated as the sum of the squared differences between the indoor air temperature of the model prediction and simulation, shown in Eqn. 16.

$$error = \sum_{1}^{n} \left(\mathrm{T}_{\mathrm{air,\,model}} - \mathrm{T}_{\mathrm{air,\,sim}}\right)^2 \tag{16}$$

The built in "fminsearch" finds the local minimum of the scalar function (Eqn. 16) of several variables, starting at an initial estimation (which was found using a large parameter sweep) over a series of iterations. The built-in function relies on the Nelder-Mead simplex method, which does not utilize derivatives to find minimum function values, but rather it just evaluates function values to determine the optimum values. Unlike the EnKF which recursively updates using new data, this approaches just requires one static set of data upon which the function looks to optimize. The algorithm runs until the area of the polytope in the solution space reaches a defined size.

3.3.5 Model-Based Predictive Control

The general objective of MPC is to be able to determine the future system response based on a manipulated variable that optimizes the future operation of a system or plant while staying in a certain acceptable set point range. In this case, the system is the automated room while the manipulated system is the blind actuation. A general approach to MPC is illustrated in Fig. 16. The plant is optimized within a limited window, the prediction-time-horizon, using only the specifics (i.e., current

temperature, solar radiation, etc.) at the beginning of the timestep (at time k) that are a result of the measurements and past control inputs (i.e., what position the blinds have been in).

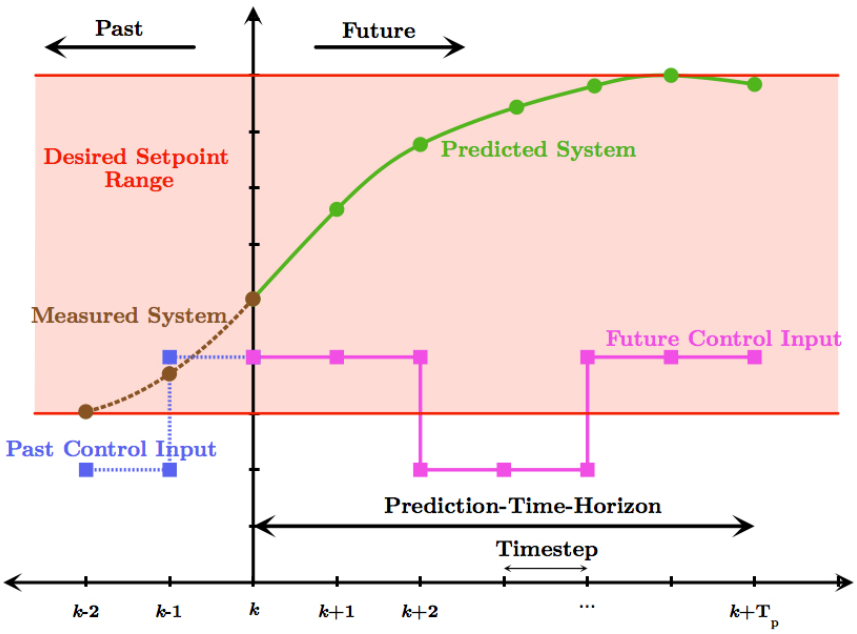

Figure 16: A general illustration of MPC.

The major consideration in the design of an MPC strategy are:

1. the model of the process
2. the known history of the past
3. an optimizing cost function (J)

The first two items are taken care of using the EnKF to train the model and the availability of data provided through the building simulations, which in this case could represent a BMS. The selection of the optimization cost function is where MPC strategies can widely differ between applications.

Optimizing Cost Function

An optimal control sequence was developed using Newton's Method of Optimization, similar to that employed by Gunay *et al.* [62]. Newton's Method is simply another method of finding the zeros of a function which could be easily implemented. In this situation the goal was to minimize the difference between the Reference System and the Predicted System (see Fig. 16). Here then the general optimizing cost function then becomes the function seen in Eqn. 17.

$$J = (R_{\mathrm{s}} - Y)^T (R_{\mathrm{s}} - Y) + \Delta U \bar{R} \Delta U \tag{17}$$

The R_{s} data vector contains all of the setpoint information (the heating and cooling setpoints), while the Y represents the vector of predicted states (what the temperature of the room will be if nothing is done). The first term of Eqn. 17 is then linked to the minimizing of the errors between the predictions and the setpoint information. The ΔU is the square coefficient matrix for the control sequence array; $\bar{R}$ is diagonal matrix containing the tuning parameters (r) that indicates how the controls should be weighted at each timestep. This second term of Eqn. 17 signifies the balance between the desire to minimize the error and the magnitude of the ΔU signal. For example, in the case that r equals zero, the optimization goal is interpreted as the situation where no attention would be paid to how large ΔU can be. The formal definition of ΔU can be seen in Eqn. 18; note the potential simplification to include the Hessian (H) in Eqn. 19.

$$\Delta U = \left(\Phi^T \Phi + \bar{R}\right)^{-1} \Phi \left(R_\mathrm{s} - Y\right) \tag{18}$$

$$= \mathrm{H}\Phi \left(R_\mathrm{s} - Y\right) \tag{19}$$

$$= \Psi \left(R_\mathrm{s} - Y\right) \tag{20}$$

The square coefficient matrix Φ is specific to the situation. The dimensions of the matrix are $\mathrm{N_p} \times \mathrm{N_p}$ and the coefficients are determined in the conversion of the system to the state-space representation. The Ψ calculated eventually becomes the weighting factor used in the calculation of ΔU. For example the first-order model expressed in Eqn. 2 and using a prediction-time-horizon of seven hours (i.e., $\mathrm{N_p} = 7$) results in the Φ seen in Eqn. 21 where $A = 1 - \frac{1}{\mathrm{R \cdot C}}$.

$$\Phi = \begin{pmatrix} 1 & 0 & 0 & 0 & 0 & 0 & 0 \\ A & 1 & 0 & 0 & 0 & 0 & 0 \\ A^2 & A & 1 & 0 & 0 & 0 & 0 \\ A^3 & A^2 & A & 1 & 0 & 0 & 0 \\ A^4 & A^3 & A^2 & A & 1 & 0 & 0 \\ A^5 & A^4 & A^3 & A^2 & A & 1 & 0 \\ A^6 & A^5 & A^4 & A^3 & A^2 & A & 1 \end{pmatrix} \tag{21}$$

3.3.6 Implemented Control Design

The entire MPC algorithm was placed into EnergyPlus using the built-in energy management system (EMS). The EMS object is a high-level controller that is able

to access a wide variety of sensors within the simulation and allows the user to implement custom control strategies over almost all of the building's systems. The complete strategy is illustrated in Fig. 17, and consisted of three main portions: (1) the predicting agent, (2) the analysis agent and (3) the decision agent. The predicting agent was responsible for the using the trained RC model to forecast the response of the building over a set prediction horizon. These trained parameters came from the offline work performed in MATLAB, because software limitations, including lack of data array structures, prevented the EnKF methods from being embedded within the EMS environment. Forecast data for solar intensity on the exterior surface and the ambient temperature were passed to EMS as a file; similar to how many BAS are now able to access the Internet for data. Forecasts were designed to be realistic and not be exactly the same as the weather used by the simulation so a random error value was included. This was to make the situation seem more plausible. The analysis agent took the forecasted thermal response and compared the predicted internal temperatures to the setpoint values at their respected timesteps. Their differences were then weighted (by Ψ) using the associated values derived in Sec. 3.3.5. The decision agent used the weighted sum to determine the appropriate control response, in terms of shade actuation. These control decisions could be based on the costs arguments but also on the potential comfort of any occupants in the space.

3.4 Numerical Investigation

With so many unknowns about the function of the designed controller a number of elements were numerically tested to get a foundation for the designs used later. The main investigations preformed are further described below.

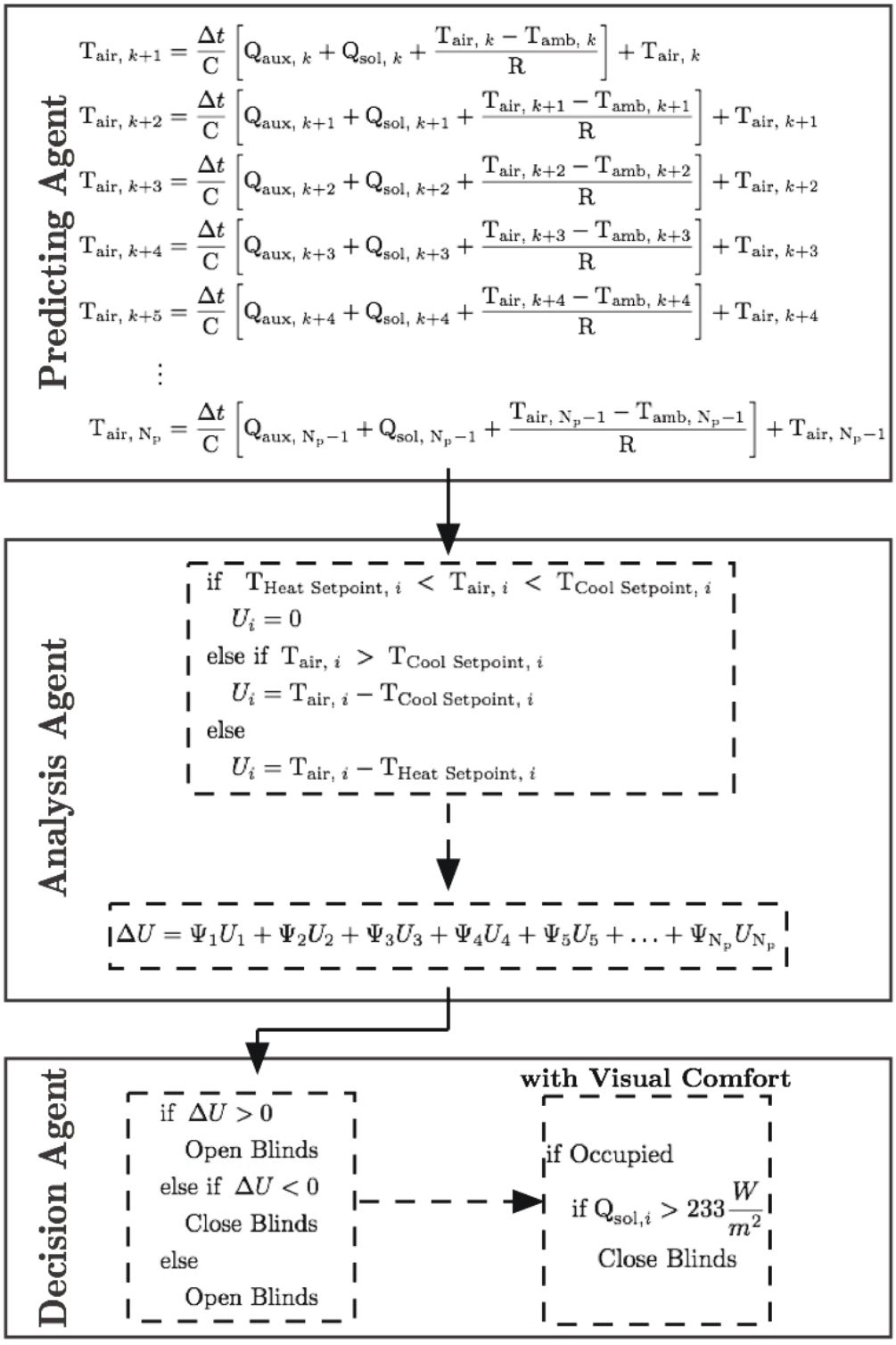

Figure 17: Implemented control method.

3.4.1 Training Conditions

Extracting performance and environmental data from the *shoebox model*, the training of the parameters in both the first and second-order models could be conducted within a MATLAB environment. The model parameters of the RC model were given as an initial estimation, based on basic knowledge, and were trained to effective values offline using the EnKF. Other researchers who have utilized Kalman Filter-based approaches, such as Radecki and Henecey [36], encountered issues in the variance values and improper convergence and needed an overlying self-excitation methodology to monitor and correct value convergence. For this reason, the training process was attempted using differing timestep lengths to understand and hopefully avoid the same issues. It is hypothesized that the shorter timestep, which will have less variance in values will be more susceptible to the same issues found by Radecki and Henecey [36] and would need to be more carefully approached or avoided.

3.4.2 Forward Modelling

Forward modelling was performed to demonstrate the effectiveness of the training methods and the simplified models at capturing the thermal performance of the building space. In order to demonstrate the capabilities, the mean value after the model had been trained for an adequate amount of time and the values were relatively stable was placed in for the parameters of the RC model. The data collected from the EnergyPlus model in terms of loads and ambient conditions was fed into the model to determine how close the RC model could determine the interior temperature of the space through the solving of Eqn. 2 and the set of Eqn. 3 and Eqn. 4. The results of the global optimization for parameter estimation were used in the comparison as the relative 'best-case scenario' for estimation and forward modelling. If the first-order

model was able to adequately capture the thermal behaviour compared to the baseline EnergyPlus results and the 'best-case scenario' then it would be the more ideal model going forward because of its easier implementation.

3.4.3 Optimization Metric

As part of the optimization construction, the value about which the system is to be minimized needs to be determined. The first logical approach would be the minimization of total electricity used by the zone for HVAC and lighting. Most researchers applying MPC strategies to building controls have used this metric. In this case, the minimization function uses equal weightings for each hour so the tuning parameter (r) was selected as 0.5.

Alternatively, some investigations have looked at the minimization of costs. Reductions in costs can be highly lucrative and much easier to sell to stakeholders because of its tangible results. Many commercial and residential settings are subject to time of use (TOU) billing. With this comes varying utility costs both seasonally and daily. In Ontario, commercial buildings who use less then 250,000 kWh and have peaks lower then 50 kW are on the Regulated Price Plan (RPP). Large commercial buildings can be charged in a similar TOU method but pay a different rate. For this reason it remains possible that reducing total utility use might not also result in lowest total monetary costs. A break down of a TOU schedule for Ontario is shown in Table 1. Rates are listed as from Hydro One [63].

Though rates change seasonally, the increased rates during the period of 7:00 am-7:00 pm (7:00-19:00) during weekdays are a constant trend. In implementation then, these hours are weighted as a higher cost to all other hours and controls

Table 1: Time of use billing schedule rates for RPP customers.

Time	Summer Season (May 1 - Oct 31) [cents/kWh]	Winter Season (Nov 1 - Apr 30) [cents/kWh]	Weekend and Holiday (Jan 1 - Dec 31) [cents/kWh]
0:00-7:00	7.2	7.2	7.2
7:00-11:00	10.9	12.9	7.2
11:00-17:00	12.9	10.9	7.2
17:00-19:00	10.9	12.9	7.2
19:00-00:00	7.2	7.2	7.2

decisions should be made accordingly. By not adjusting further for the seasonal differences, any potential controls are much easier to implement, as a seasonal switch in setting is not also required. To accomplish this decision weighting, the tuning parameters were required to be adjusted for each prediction-time-horizon length. With the cheaper hours being weighted as 0.25 and the higher rates at 0.75. The weighting values are fairly arbitrary, since in the weighted sum the values become normalized. The critical aspect (compared to the previous design which had everything weighted uniformly at 0.5) was that the values were different and skewed for more expensive hours to a higher value. Since, as was previously mentioned, a weighting of zero gives an absolute setpoint with no discretion for the energy required to keep it there. The lower priced hours should be closer to this condition then the peak-hours.

Other utility pricing schemes could lend itself to predictive control strategies. One example of which is the pricing of the utility based on a peak value over a certain time interval. The method here was not set up to be directly transferable to situations such as this. These would most likely require the forecasting of a prolonged period or would require the continual checking of peak values forecasted in the short term

and compared to a historic log of past peaks.

3.4.4 Prediction-Time-Horizon Length

A consideration with any predictive strategy is the length of time to look ahead and base control decisions. In this MPC, a *receding horizon* strategy was employed. In this scheme only the first timestep's control decision was implemented but the optimal strategy over the entire prediction-time-horizon was still sought. If too small a time horizon is considered, the thermal capacitance will not be fully utilized. Yet, if too long a prediction-time-horizon is considered, decisions become more effected by errors in forecasts, models and increased computation effort. It is then ideal to find the right balance in lengths. The optimal prediction-time-horizon is situationally independent, and is a function of the properties of the space. For example, the larger the thermal mass the longer the required window. In order to investigate this numerous simulations were run with varying prediction-time-horizon lengths to determine an adequate length for control in this situation.

Chapter 4

Results

4.1 Numerical Investigation

The numerous research questions outlined in Chapter 3 were explored. Investigations initially started numerically using the first-order model of the simulated building space. The performance of the first-order model was compared to a second-order model in key design considerations. Finally these results were transferred to the control of a physical space in a demonstrative situation.

4.2 Parameter Training Results

4.2.1 First-Order Models

Global Optimization

Initially, the first-order model was trained using a global optimization technique (outlined in Sec. 3.3.4). The values found through this method are listed in in Table 2. These are considered to be very near the best estimate of the values for predicting the thermal behaviour of the modelled space. The fit of these parameters between the

training data and the fitted model can be seen for an 84-hour period in Fig. 18. The RMS error value of this fit had an RMS error of 1.5°C. It can be seen that the trained model responds slower to changes then the modelled space, as such it does not hit the same maximum and minimum values as the shoebox model. The result is related to the effects of heat transfer not captured in the process between the thermal mass and the rest of the space. As a result the thermal mass to charges and discharges less effectively.

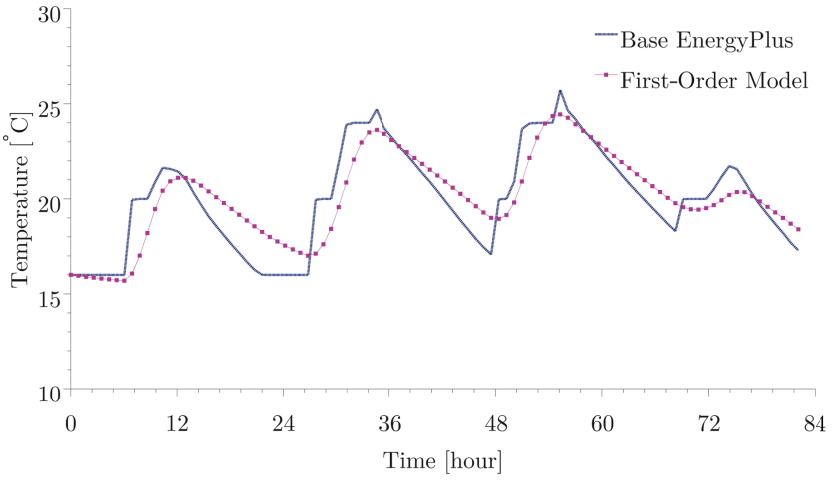

Figure 18: An example of the first-order model training using global optimization over an 84-hour time period.

Table 2: Global optimization minimum search.

Component	Unit	Value
C	$J \cdot^{\circ} C^{-1}$	8.694×10^6
R	$^{\circ}C \cdot W^{-1}$	0.057976

The inability of the model to fit better to the training data is a result of the simplifications that a first-order model places on the representation of the zone. Many of

the advanced heat transfer process at work in conditioning the space are not captured in the training data. For example the changing infiltration or exfiltration of the space is not considered. These data sets could have been reported out of the *shoebox model* however it would be unreasonable to have this sort of information in a standard BAS. It could have been estimated based on a schedule or consistent value but this was viewed as being too ideal a set of knowledge and too far from many actual building control situations and too reliant on a very informed individual.

EnKF Training

The use of the EnKF to recursively train the parameters was more novel than the global optimization method but had elements which, based on similar approaches by other researchers, were of particular interest. Firstly using a 30 minute timestep the values of R and C converged to those values seen in Table 3. Being ensemble values, they are represented as a Gaussian distribution expressed as a mean and variance. Since the values were trained for such a long period of time the variance value evolved down to a very small value, when compared to the mean. If the value were to continue to decrease the system would run into operation issues and would potentially need to be artificially perturbed. The system being trained from however was very static compared to real-world situation which would help prevent this issue in practice.

Table 3: First order model EnKF converged values using 30 minute timestep.

Component	Unit	Value	Variance
C	$J \cdot^{\circ} C^{-1}$	8.0227×10^{6}	2.885×10^{-6}
R	$^{\circ}C \cdot W^{-1}$	0.045	5.02×10^{-10}

The resulting values based on the EnKF were found to be similar to those found

by the global optimization (Table 2). The nature of the system being classified means that there are multiple possible combinations that result in a similar level of accuracy. As can be seen in Fig. 19, there are many combinations of R and C that result in minimized errors of the same magnitude. The apparent movement of the ideal combination through seasonal changes illustrated in the differences between Fig. 19 (a), (b), and (c) further illustrates the need for a recursive strategy for any system looking to capitalize on a simplified thermal model. This parameter shifting is most likely related to simplifications made within the modelling of the system but also the relationship in the values to different environmental conditions. For example, the thermal resistance (and consequently conductivity) is a function of the temperature while the capacitance value is a function of the relative humidity. Depending on where the models start from in progression towards the minimized region numerous different values could be converged to even if using the same methodology. Though problematic in defining a 'correct answer' it means that in terms of building controls a large range of values are potentially acceptable to the training and implementation of parameters.

In order to explore the potential limitations of the method when perturbations to the system were differing, the timestep length between data points was adjusted from one minute to one hour at various intermittent durations. The progression of these values for the resistance value (R) is illustrated in Fig. 20. As can been seen most timestep lengths evolved to a similar value when starting at the same condition and given the same 5000 timesteps. The only exception to this being the one-minute timestep, which if given more timesteps would most likely eventually achieve a similar value. This is indicative of the problems incurred by Radecki and Henecy [41] in which a system had convergence issues. Later Radekci and Henecy [36] determined

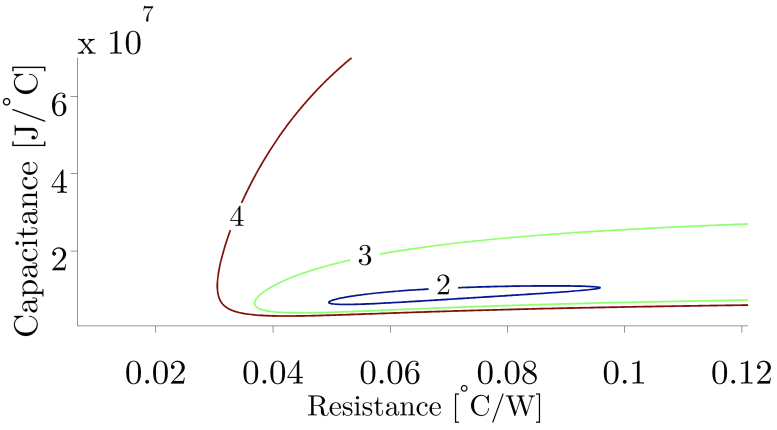

(a) RMS error in Winter

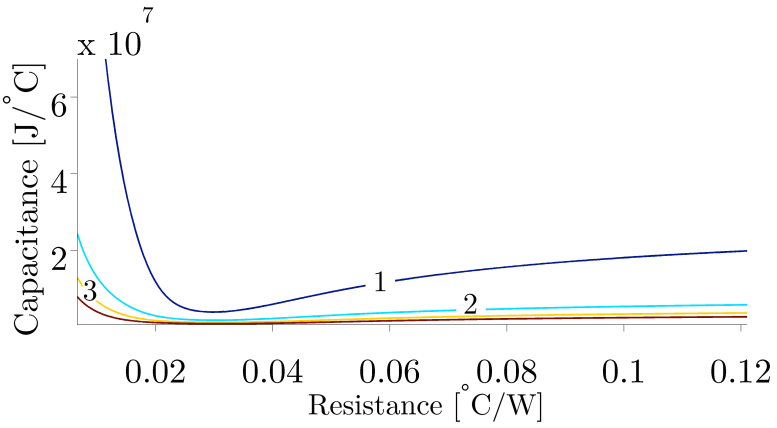

(b) RMS error in Summer

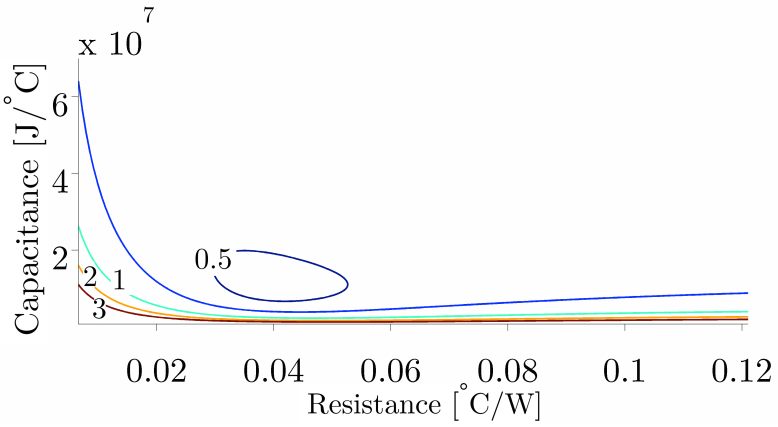

(c) RMS error in Fall

Figure 19: Error contours for a 24-hour period at different times of the year.

this was a result of not enough perturbation to the system during training. This same issue would be experienced by the one-minute timestep with there not being enough difference between the measurements of the state between timesteps to drive the system as effectively. They solved this issue using a perturbation function during ideal times in building operation. The opposite effect can be seen in the initial evolution of values shortly after initialization in Fig. 20. The longer timestep lengths (i.e., one hour or 30 minutes) initially move much faster to evolve, seen as the faster rise in values. In practical applications though a one-minute timestep is not required and could actual be detrimental to system performance depending on the network configuration and the quantity of data already being sent through the network. This hardware limitation become problematic in efforts to access many aspects of current BAS systems.

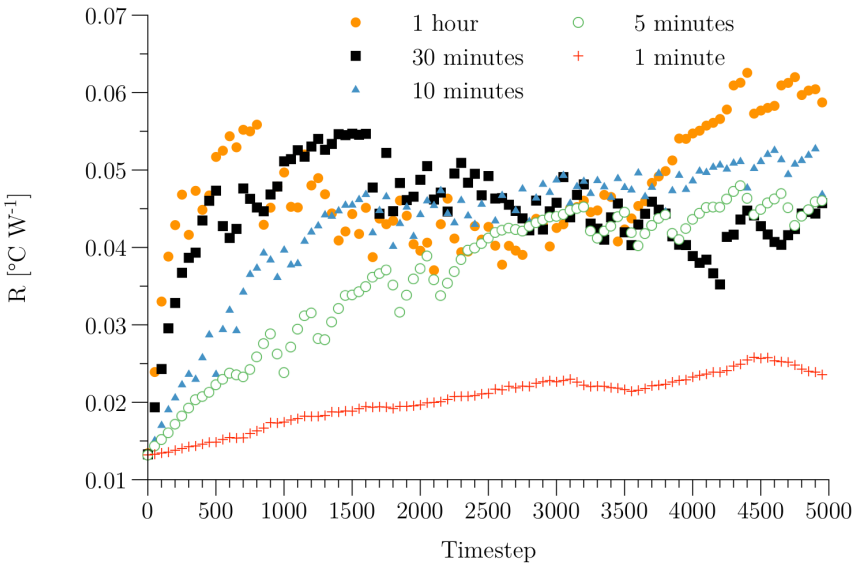

Figure 20: Parameter estimate evolution for first-order model.

4.2.2 Second-Order Model

The training of a second-order model was attempted. Using the same 30 minute data as for the first-order model, effective values for all the parameters were found to be those in Table 4. The converged values for the second-order model are more difficult

Table 4: Second-order model EnKF converged values using 30 minute timestep.

Component	Unit	Mean Value	Variance
C_w	$J \cdot^\circ C^{-1}$	8.72×10^5	2.61×10^3
R_w	$^\circ C \cdot W^{-1}$	1.65	2.76×10^{-4}
C_{air}	$J \cdot^\circ C^{-1}$	7.84×10^6	2.41×10^3
R_{air}	$^\circ C \cdot W^{-1}$	0.51	2.33×10^{-5}

to validate. A global optimization is difficult to accurately train with four parameters as there are a significant number of potential combinations that give similar results. Secondly, being effective values, it is difficult to split the material properties and calculate the values. One aspect of note in the converged values are the high variance on the capacitance values. This is partially a result of the wall temperature only being forecasted and never actually measured. Meaning that this state is always very uncertain. As the capacitance value of the wall is subject to high variability so to is the capacitance of the air node, since so many combinations of these values will result in reasonable results. This high uncertainty of a non-measured state would be nearly impossible to apply in training methods such as a least-square or recursive least-square as in these methods knowledge of states is assumed to be known and nearly ideal.

The capacitance value for the interior node in comparison to the relative capacitance of the air in the space was found to be approximately 100 times larger in both

instances. The effective values found by the recursive training accounts for the air and the construction materials, which is why the value was found to be larger.

4.2.3 Forward Modelling Results

The forward modelling was intended to gauge the validity and abilities of the building model parameter values. Using weather and auxiliary load data, which was not used in the training interval, the indoor air node's temperature was forecasted using the various trained model and compared to the simulated environment in EnergyPlus, as seen in Fig. 21. The 24-hour forecast illustrates the model abilities and shortcomings but the 1-hour forecast repeated each hour over a 24-hour period is more in line with the conditions in the controller as after each timestep the predictions were recalculated.

The associated RMS errors for the plots in Fig. 21 are contained within Table 5. As can be seen there is a considerable decrease in the values in the associated errors between the two different forecast lengths. More interesting is the increased error of the second-order model relative to the first-order model as trained using the EnKF. Partially explainable by the higher uncertainty in the values meaning the values were better trained in the first-order model. A secondary issue could be the lack of a steady state value being achieved in the wall node over such a short period (i.e., there is an insufficient burn-in period). This is a potential implementation issue when being used in a consistently refreshed model of the system.

Based on these results, the abilities of the first-order model were deemed to be sufficient for the required model as part of the MPC. Ultimately the added complexity of the second-order model did not provide a similar increase in the accuracy of the predictions.

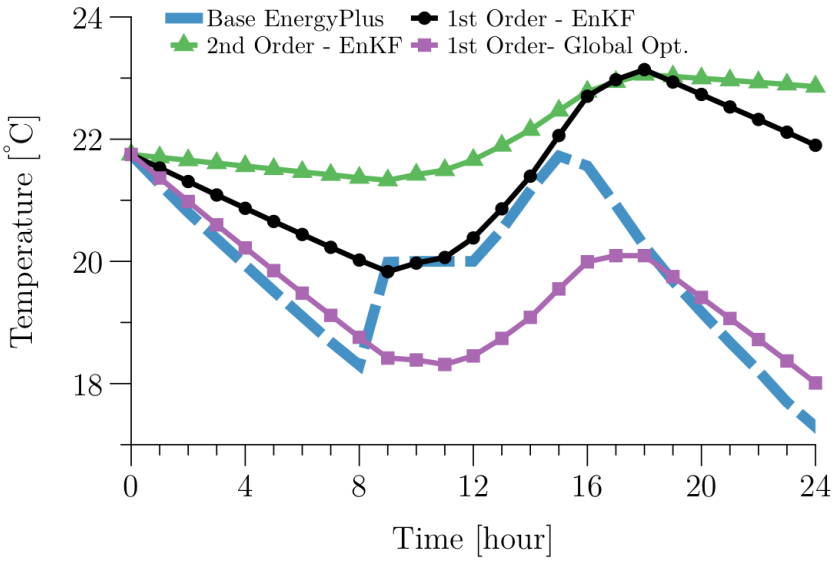

(a) 24-hour forecast

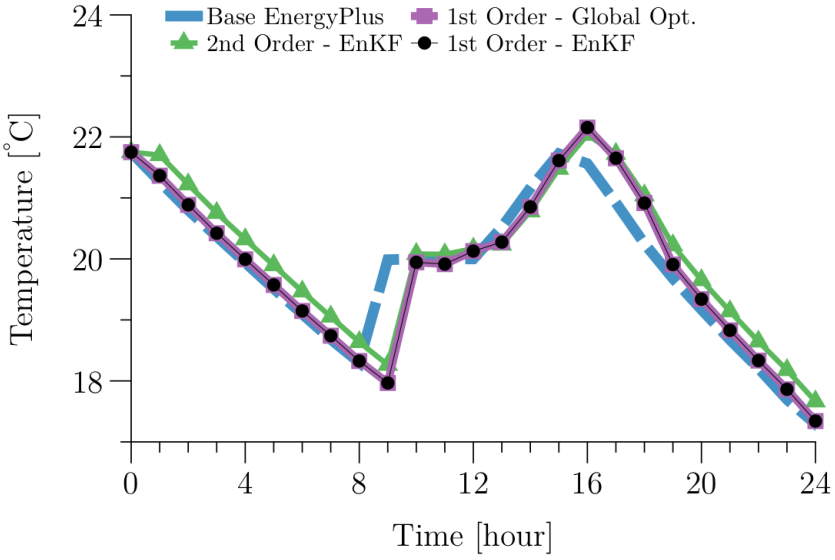

(b) 1-hour forecast

Figure 21: Forecasting comparisons for 24 and 1-hour ahead.

Table 5: Calculated RMS error values from plots in Fig. 21.

Training Method and Model Type	24-hour forecast RMS error [°C]	1-hour forecast RMS error [°C]
EnKF First-Order	2.193	0.520
EnKF Second-Order	2.696	0.540
Global Optimization First-Order	1.058	0.481

4.3 MPC Elements

Prediction-Time-Horizon Length

The aspects of the prediction-time-horizon length were tested to determine the ideal length for the building model. Numerous simulations were run using the total electricity minimized controls and various lengths of the prediction-time-horizon. In each run the cumulative heating and cooling loads were compared to that of the baseline model. The results for three of these prediction-time-horizon lengths are shown in Fig. 22 as cumulative energy usage for both heating and cooling. As can be seen, as the time length change so too do the loads. Further, and expectedly, as the heating loads increases the cooling load decreases. Under a 7 hour prediction-time-horizon, the baseline reactive system has either an advantage in cooling or heating loads, as seen by the offset between the curves. Extending the horizon up to 9 hours in length did not result in significant energy savings (if any) so 7 hours was deemed to be ideal length going forward. The cooling loads were found to be the more susceptible of the two to the prediction-time-horizon variation. Unlike the heating electricity usage, which saw benefits with all timestep lengths, the solar gains are not advantageous. No matter when they are added it is still a benefit to zone. The cooling energy usage is dependent of the delayed thermal effect of the solar gains. The selection of

optimal lengths was found to be a very under-discussed topic within the literature on predictive controls.

4.3.1 Optimization Strategies

The MPC control strategy in the *shoebox model* was implemented using two different optimization strategies. This allowed for a comparison as to whether it was more beneficial to optimize for electricity use or cost. The total heating and cooling electricity and costs are presented in Fig. 23.

It is noticeable that using either optimization method provides similar savings either in electricity or total cost at 34% and 38% respectively. The majority of the savings come from the heating system over the baseline that, especially during the winter months, would have the blinds closed for long periods of the day rejecting the useful solar gains. The increased savings in cost compared to the electricity use is indicative of the time in which much of the savings occurred. Since the majority of benefits (both in terms of solar gains and rejection at the correct times) occur during the daytime hours when costs of electricity are higher.

The actual energy consumption used by the both cost function methods is compared to the baseline once again in Fig. 24. The figure shows that in actuality the energy consumption in the space when using a method biasing for TOU does not result in a different amount of energy being used by the heating and cooling system. The TOU method has only two times of transition upon which controls should be heavily weighted to times of cheaper energy rates. These two times (7:00 am and 7:00 pm) occur at times when solar gains are not major considerations of the system so shade actuation did not vary drastically. Had this control been actuating an HVAC system in which more modulation was possible (and not just a binary on/off) such as

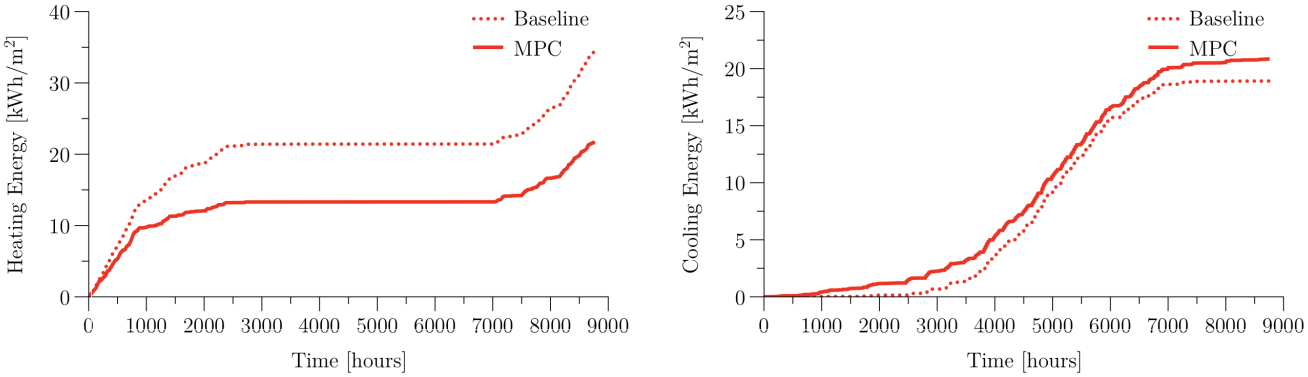

(a) Loads with 5 hour prediction-time-horizon

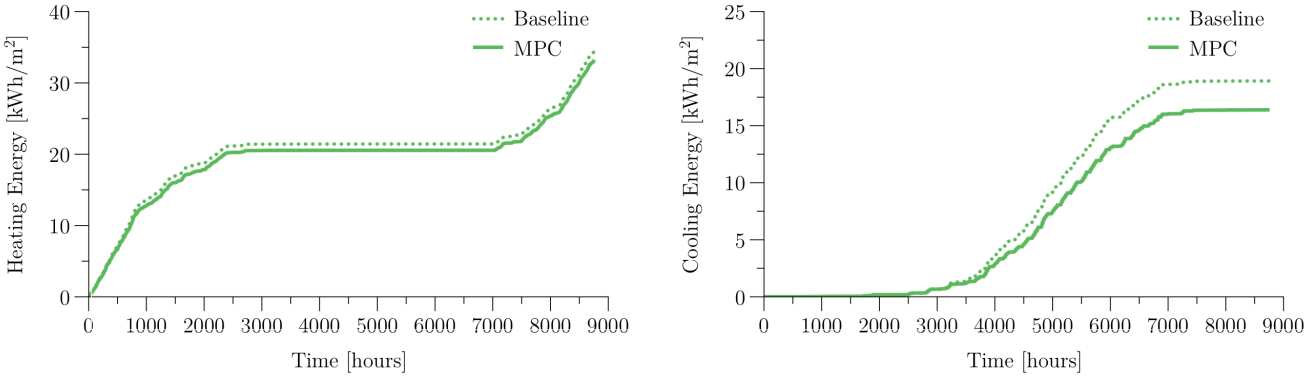

(b) Loads with 7 hour prediction-time-horizon

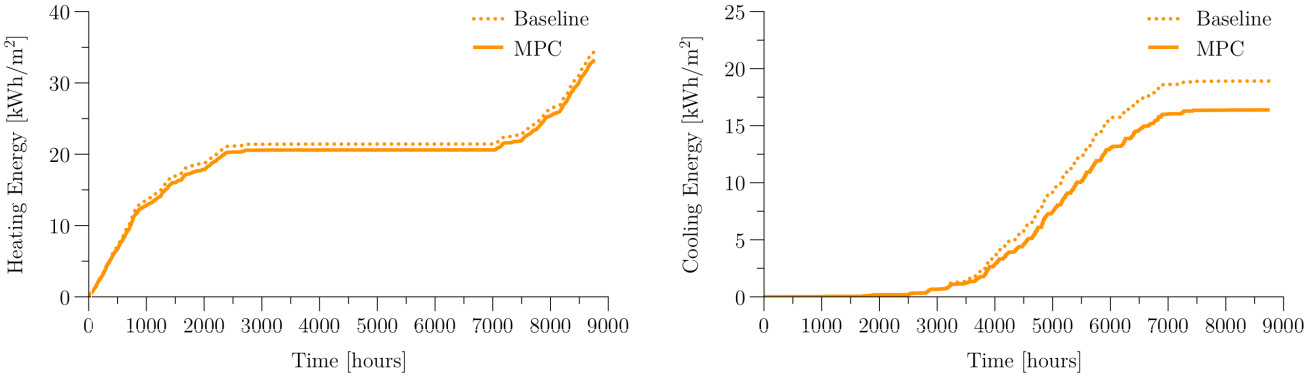

(c) Loads with 9 hour prediction-time-horizon

Figure 22: Cumulative heating and cooling loads.

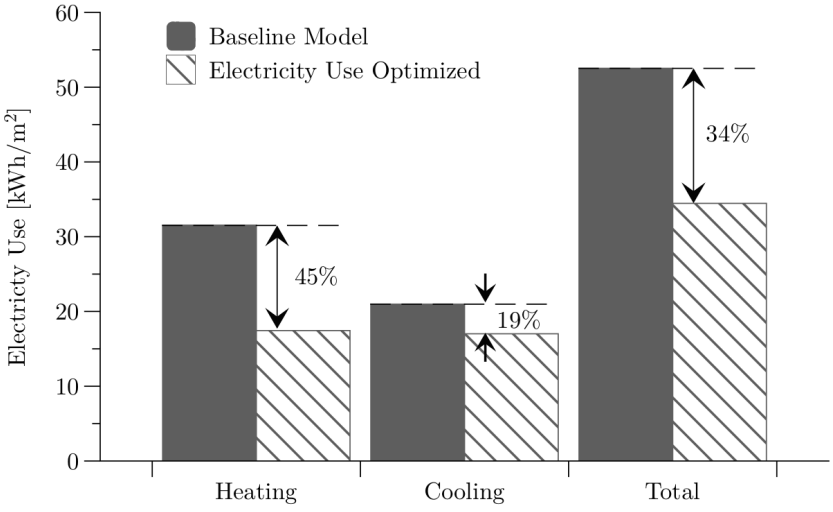

(a) Total heating and cooling electricity use.

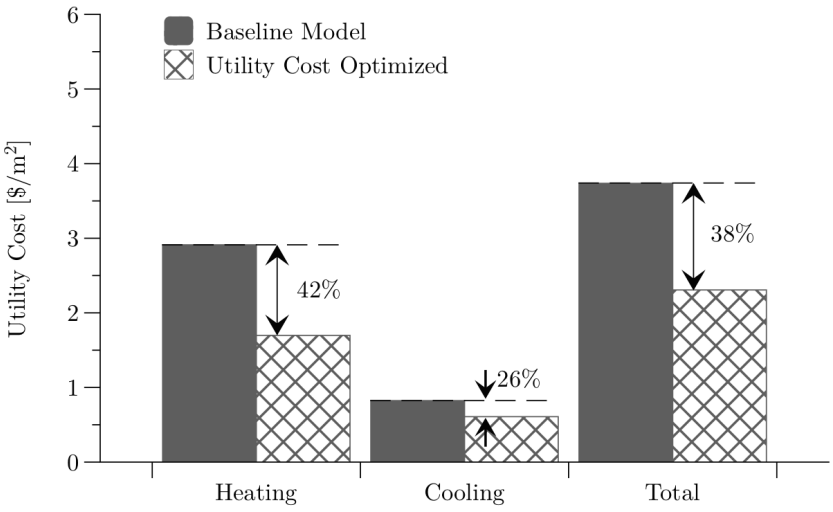

(b) Total heating and cooling electricity cost.

Figure 23: Comparison of optimization cost functions.

in Ma *et al.* [30,31] or the OptiControl project [23] there would have been expected a larger distinction between strategy choice.. This system did not look at the altering of the lights within the space, which in the *shoebox model* were on during occupied hours and represented another 21 kWh/m^2 and could be the potential for significant further savings in systems that had lights controllable by the BAS.

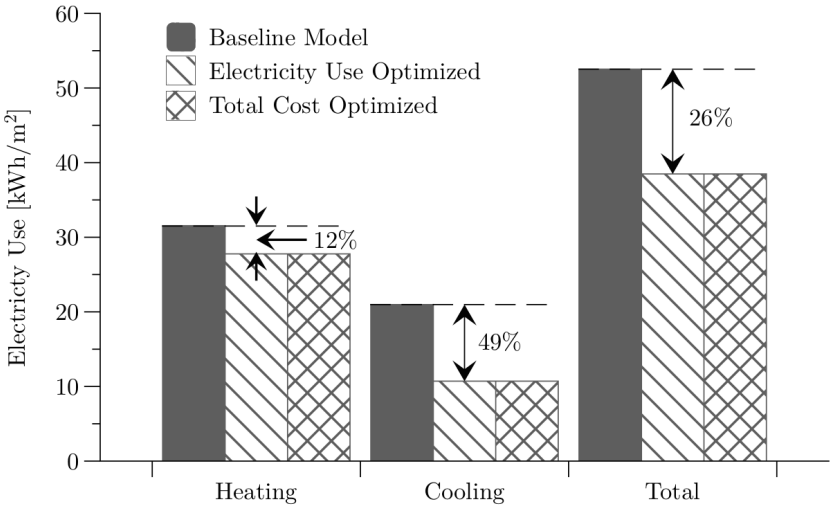

Figure 24: Electrical energy use by both optimiziation methods compared to the baseline.

Systems Extensions into Lighting

An extended aspect of the optimization strategies looked at the inclusion of a visual comfort criteria within the Decision Agent portion of the controller. Though not controlled explicitly by the MPC approach, the inclusion of visual criteria is essential to developing a system that occupants are willing to accept. Further it is possible in many BAS to control the lighting. For that reason it could be automated along with other elements within the space. As can be seen in the Fig. 25, the energy usage by the heating, cooling and lighting of the space is tabulated once again optimized either for cost or energy but now allowing for the lights to be turned off automatically

if the shades had been closed for visual comfort reasons. As can be seen with both strategies, the heating loads increased and cooling loads decreased, a result of the decrease in lighting use in the space which contribute to the heating load. This approach adds more potential savings for the building operators over the baseline model.

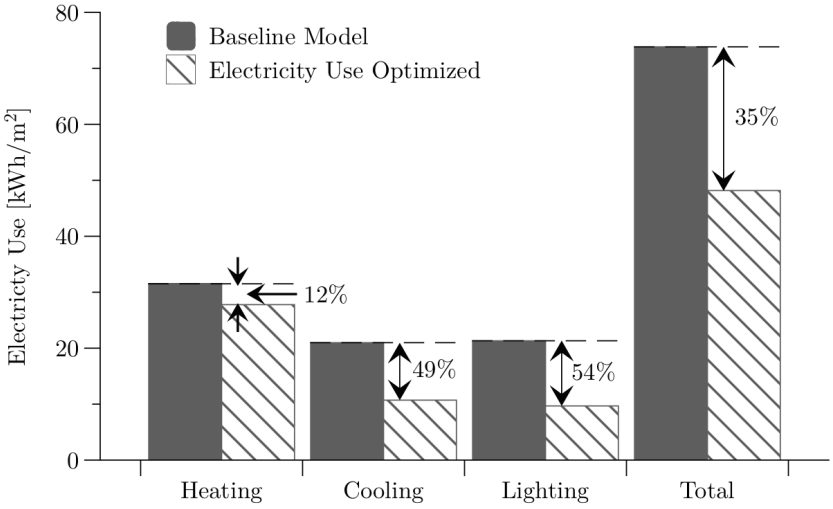

(a) Total heating, cooling and lighting electricity use.

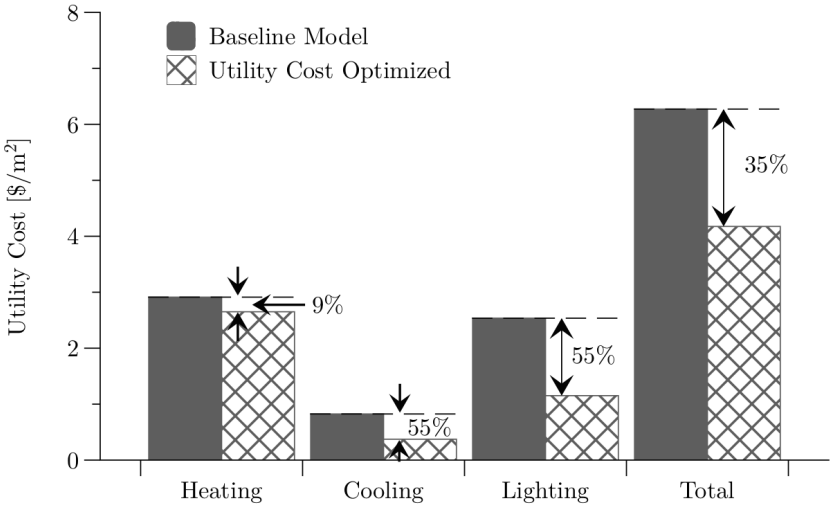

(b) Total heating, cooling and lighting electricity cost.

Figure 25: Comparison of optimization strategies when including visual comfort.

Chapter 5

Demonstration Facility

5.1 Introduction

The control algorithm was implemented in a physical space, less to fully utilize the system developed through simulation and numerical work in Chapter 3 and more to attempt to implement a system based off of the lessons learned during it. The goal was to develop a system, appropriate for a standard BAS and address challenges and problems of incorporating a system that interacted with a building and its occupants.

5.2 The Delta Controls Lab

A demonstration facility was developed in the Delta Controls Lab of Carleton University. The 12 m^2 office is located on the western edge of the Carleton campus; see Fig. 26(a). The space has an approximate southwest orientation with three large windows on only one wall and a window-to-wall ratio of 60%. The space is conditioned with two overhead radiant panels fed by hot water lines from a centralized heat plant on campus and two air diffusers which deliver neutral temperature air in the heating season and conditioned air during the cooling seasons. The office is regularly occupied

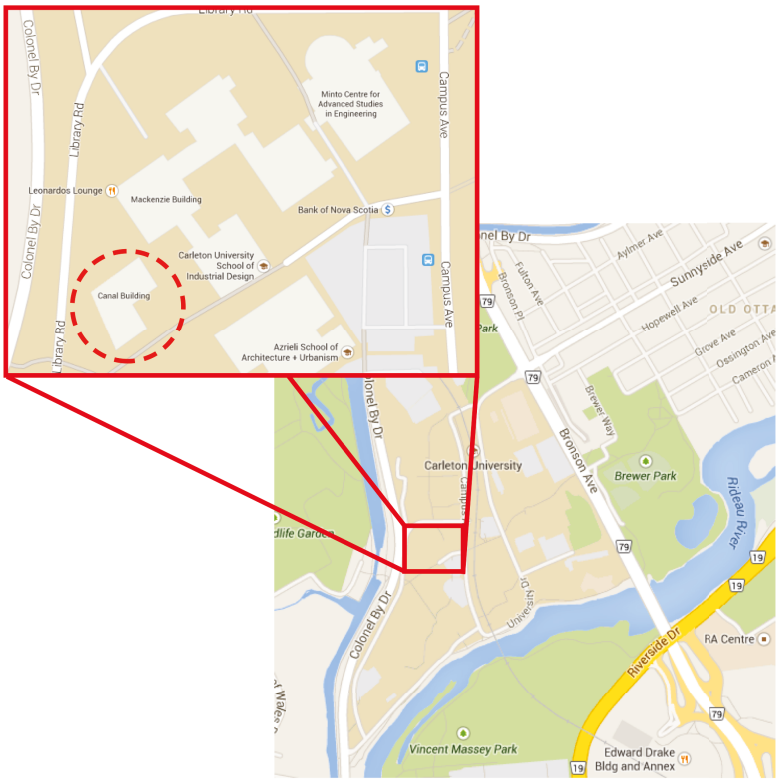

(a) Physical Location

(b) Elevation and Layout

Figure 26: Delta Controls Lab overview

by up to five graduate students who keep a fairly consistent occupation level from 7:30 am - 6:00 pm. Outside of these times the office is usually unoccupied. Three non-dimmable lighting fixtures each with two fluorescent bulbs provide overhead illuminance. The operative temperature strategy of the room was not changed from the static setpoint style the room had previously been controlled under. The setpoints were found to be a very narrow operation band and were adjusted to have a heating setpoint of 21°C and a cooling setpoint of 25°C. Though not ideal for both heating and cooling seasons simultaneously, they fall within seasonal limits of comfort as defined by ASHRAE Standard 55 [64].

5.2.1 Facility Setup

The number of adaptations to the space for this investigation was kept to a minimum. Realistically the more changes to a standard office space, the more the incurred cost by building owners and the less likely they will be undertake a project of this nature. The existing roller shades were retrofitted using Somfy Sonesse RTS 30 motors (Fig. 27(a)) connected wirelessly to the BAS using a Somfy dry contact device (Fig. 27(b)). A Delta DSC-1146E, a commercially available building controller, was installed so automation of the zone's VAV, radiant panels and shades could be handled by the experimental system and not require access to the rest of the Canal building's controls. The installed system is shown in Fig. 28. Two ceiling-mounted analog photodiode sensors were installed and connected the room controller (the DSC) to monitor interior lighting conditions. A 10k thermister was placed in the plenum near the radiant panel's pipes to be used in fail-safe applications to make sure there was no risk of pipes freezing from control errors.

(a) Sonesse RTS 30 motor

(b) Dry contact device

Figure 27: Somfy hardware used for shade controls.

The only exterior data provided to the room controller was the outdoor air temperature (OAT) that was already delivered to controllers through the existing BAS. In addition to the OAT, environmental conditions were logged using a weather station installed on the roof of an accompanying building and shown in Fig. 29(a). Measurements of horizontal solar radiation, along with outdoor temperature and vertical solar radiation at the same orientation as the Delta Control Lab's windows were logged at 15 minute intervals. To measure the transmitted solar radiation, Onset silicon pyranometers were positioned just on the inside of the glazing as well as just behind the blind as shown in Fig. 29(b). These pyranometers were not able to be connected to the BAS and were removed when long-term testing had begun as they had a unique adapter to the data logger. It was attempted to find pyranometers which could be connected to the controller, however it was difficult to source ones which gave a high enough voltage reading to be compatible.

Figure 28: Installed BAS in the Delta Controls Lab.

5.3 Investigation

The demonstration facility was designed for continuing studies whose scope far exceed what was done in this investigation. The main investigations preformed were the commissioning of the system and determine the relative effectiveness of an implemented MPC design.

5.3.1 System commissioning

Besides the physical connections to devices, the system had a number of control programs that needed to be developed on the BAS for fundamental operations. With no connection between the BAS and an exterior data source (such as the weather station or the pyranometers) the predicted shading controls needed to rely on two ceiling photodiodes for a host of data. As such the sensors needed to have relations derived which directly correlated the solar flux into the room to that of the average ceiling illuminance. In this way the BAS would be able to estimate the flux of energy

(a) Weather Station (b) Pyranmometers

Figure 29: Enviromental condition monitoring equipment.

into the space in order to predict the space's response.

5.3.2 Effectiveness of an implemented control scheme

The implemented control strategy here blended the work done in the simulation work in Chapter 3 with the work of Gunay *et al.* [62] and adjusted it for the application in a less ideal environment. Following these ideas, the need for complete hourly forecasts was removed and instead the notion that current conditions could be linearised over the control horizon was attempted. A control scheme was implemented in the DSC using the native GCL+ programming language (the full code can be found in Appendix C). The control sought to be a total control solution and not just one that would be implemented during certain times. As such conditions in the controls for night time (when solar gains are not possible) and the design to place occupant comfort as the paramount concern were introduced. During occupied hours, the control sequence was implemented as is illustrated in Fig. 30. The non-occupied hours were

controlled using a much simpler Decision Agent in which the blinds were controlled strictly on thermal merits; which often is their utilization for a small increase in the insulating properties of the space while lowered. The MPC strategy is the same as was presented in the Fig. 17. The controls were implemented in the Delta Controls lab starting in March 2014. Intending to be a long-term test situation both at effectively managing the expectations of the occupants both visually and thermally while attempting to reduce the energy consumption of the zone. Occupants were given control override abilities over the system as the testing progressed. However, in the quantification of the effectiveness energy and cost (less objective metrics) were selected for analysis. For this reason, along with allowing for better management of the internal loads, most energy-based analysis took place on weekend hours and was compared to the use by a neighbouring office. The use of HVAC along with the interior temperature of the space were recorded and compared to that of physically similar office spaces down the hallway which could be monitored through the existing BAS. The comparison was designed to quantify the potential savings of the implemented shading system over an unaltered space.

5.4 Demonstration Facility Results

5.4.1 System Commissioning

The system commissioning was a critical step because the Delta Controls lab was taken off of the existing BAS and placed on its own. The entire operation of the zone was no longer being managed by the professionally commissioned system and any design failures could potentially do serious damage to the HVAC system of the zone. For that reason particular care was placed on the development of the fundamental

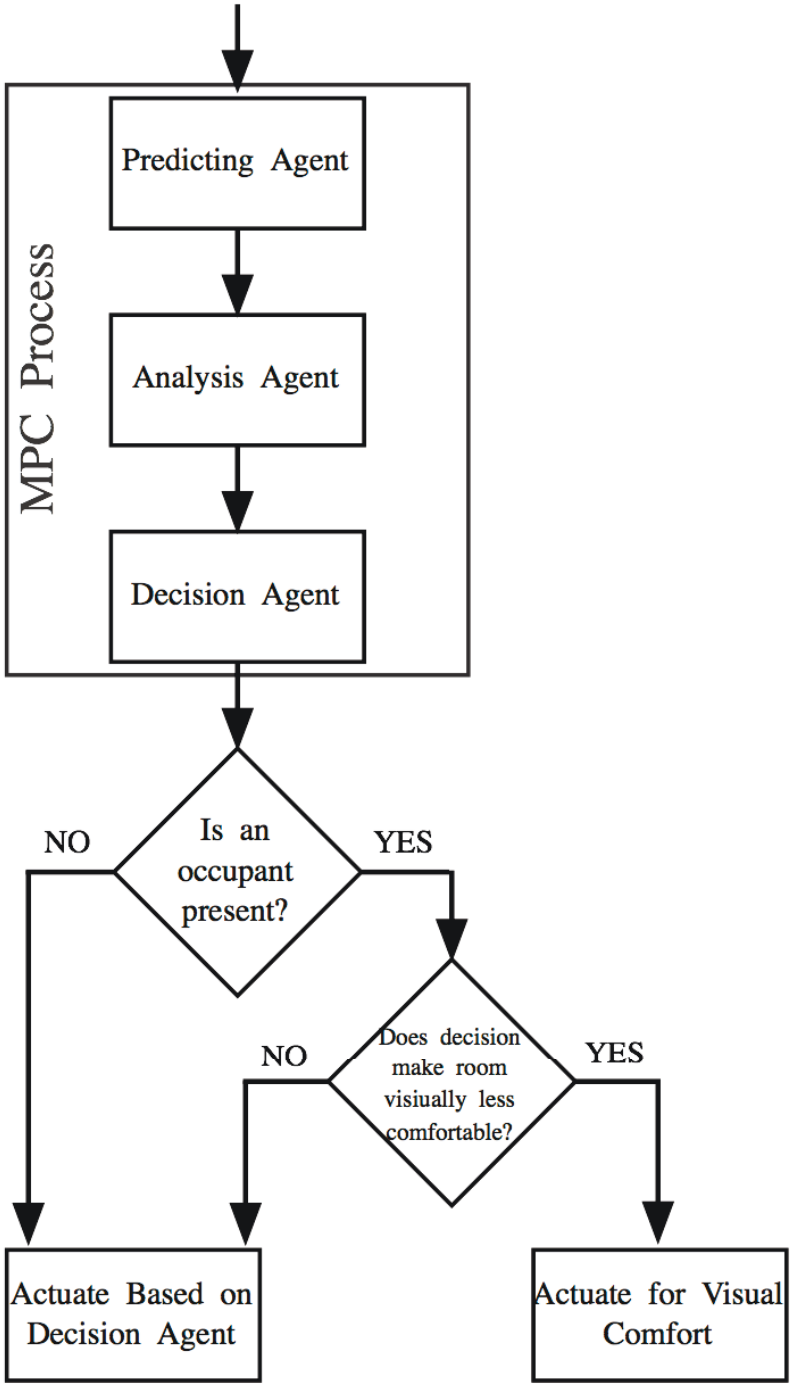

Figure 30: Daylit hour control process.

operations and fail-safe protocols were installed before any of the more advanced shading controls could be implemented.

The first of these custom systems was the correlation of the lighting conditions in the space. Using the pyranometers and installed photodiodes a series of measurements were taken relating the transmitted solar to the illuminance on the ceiling. This relation is shown in Fig. 31 along with the linear regression fit. The value of $0.1655\ \mathrm{W \cdot m^{-2} \cdot ft\text{-}cd^{-1}}$ was utilized as the conversion factor within the room's BAS system to relate the rooms measured illuminance to get a sense of the transmitted radiation through the window. The fit (based on the $R^2 = 0.6648$) is not particularly high but its partially a result of the location of the sensors on the ceiling; which protects it from any direct solar radiation on the window. Further the value for illuminance was based on the average of two sensors; one of which is located behind more obstructions due to the furniture positions. Though potentially something that could have been adjusted, it represented a real situation in an office space where occupants have created a environment that is non-ideal for the operation of a building automation strategy.

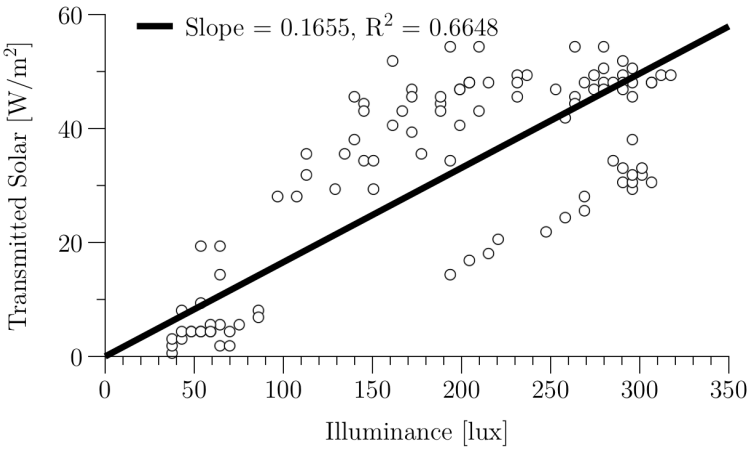

Figure 31: Illuminance and transmitted radiation relationship.

As part of the predictive system's approach an R and C estimated value were required. Ideally there would have been opportunity to train this using the recursive EnKF approach developed earlier as part of the room's developed BAS but due to constraints including the data processing rates, values were embedded within the controller following offline calculations. The values used by the BAS are shown in Table 6.

Table 6: Demonstration facility values.

Component	Unit	Value
C	$J \cdot^{\circ} C^{-1}$	2.16×10^6
R	$^{\circ}C \cdot W^{-1}$	0.05

The values are similar (in the same order of magnitude) to the values found using the various methods in the simulation investigation, but of course that was a different building. This offline approach to the parameter estimation would represent a fairly accurate situation in any advancements of this system to more commercial spaces. Starting with a reasonable value in the controller, a recursive method could then be implemented in order to update the thermal parameters and account for any change of conditions.

5.4.2 Occupant Comfort

Occupant comfort was a major concern of the automated blind system, especially since historically it is on this front that most automated shading systems are found to be lacking. In the use of a primarily visual based system for thermal performance needs, the visual aspects still need to be a constraint.

Thermally, the space was well controlled, as is shown in Fig. 32. With the implementation of the controls it can be seen there was generally a decrease in temperature fluctuation, particularly around the heating setpoint. At the time occupants had complained about the room being too cold. Part of these generally warming conditions would be the changing of seasons; however upon looking at the outdoor air temperature during that time (as seen in Fig. 33) the temperature remained fairly consistent during the two time periods. A major complaint of the initial control was the lack of any occupant-based decision (something that had been intended to be included in a refinement of the controls). With its controls there was a marked change both in the temperature profile of the room but also the amount of time in which the shades were closed (illustrated in Fig. 32 and Fig. 34, respectively). The temperature had more fluctuation within the thermal comfort range but members of the office community typically were more accepting of the control strategy. The shade data and radiant panel data (Fig. 34 and Fig. 35) only were measured after the system had been commissioned. However from the switch to include visual comfort (i.e., the data in the grey) shade occlusion was dropped from 71% to 30%. The radiant panel also had a decrease in usage, however that was partially attributed to seasonal changes to warmer temperatures around that time.

5.4.3 Energy Reduction

Energy reduction comparisons were made during the monitoring of the zones over weekend periods; a time in which the interior gains were minimal. The control setup in the Delta Controls Lab was compared to a similar office space on the same floor and with the same orientation. Data points were limited by the existing BAS for the

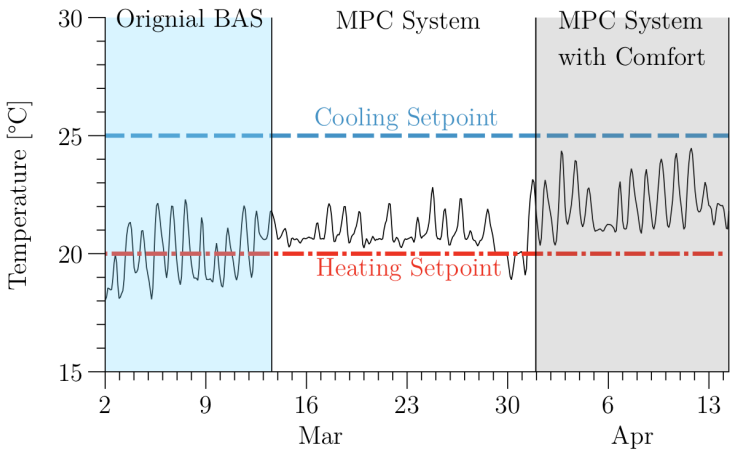

Figure 32: Indoor temperature of the Delta Controls Lab.

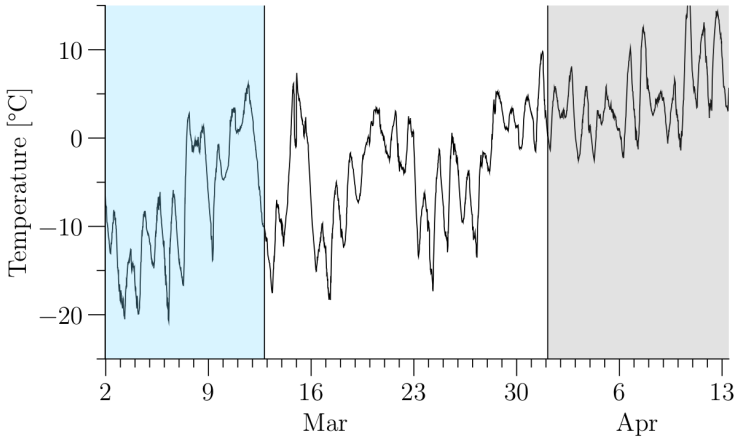

Figure 33: Outdoor temperature of the Delta Controls Lab.

other room but conclusions could be drawn nonetheless. The data collected on the sample office and the Delta Controls Lab are contained within Fig. 36 and Fig. 37 respectively.

Notably in comparison of the two spaces are the complete differences in shading position. The sample space had the blinds closed for the weekend, a common occurrence where the occupant did not open blinds when leaving at the end of day, while the predictive system had the shades open the entire time. This is the same

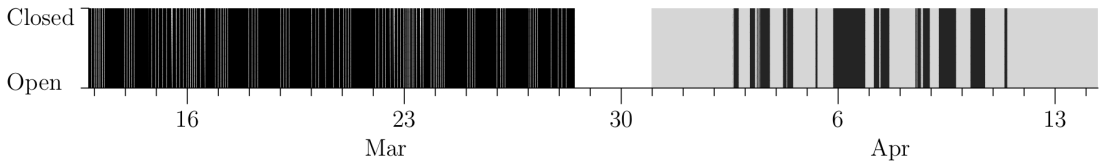

Figure 34: Shade position in the Delta Controls Lab.

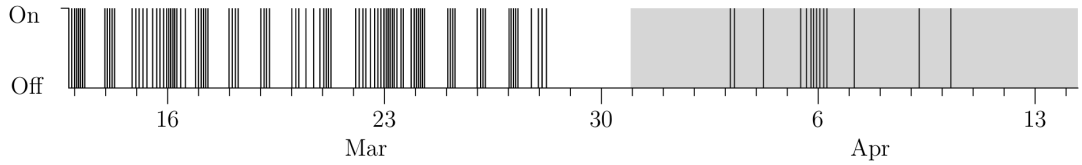

Figure 35: Radiant panel function in the Delta Controls Lab.

phenomena observed by Haldi and Robinson [65]. The lack of shade movements by the predictive system are a result of the indoor temperature never falling low enough for the system to forecast the need of heating. This approach resulted in a complete non-requirement of heating energy by the radiant panels. At the same time, the room did not overheat during the daytime as the ventilation rate never increased above the baseline ventilation rate.

In a straight comparison then, the predictive system appears to save a significant amount of energy but much of that had little to do with optimal shading positions and more with shortcomings in the existing control methodologies and controls. As can be seen in Fig. 36 the system was trying to keep the temperature between 20°C and 22°C, which is a smaller temperature band then was allowed by the predictive system, but during an unoccupied weekend could be considered extremely conservative. Secondly as can be seen in the fluctuations of the temperature, are what appear to be a small dead band. As a result the system is subjected to a periods of repeated on-off switching. In some instances, such as just after 12:00 pm on April 27 in Fig. 36, a significant spike in system ventilation will immediately follow a heating action.

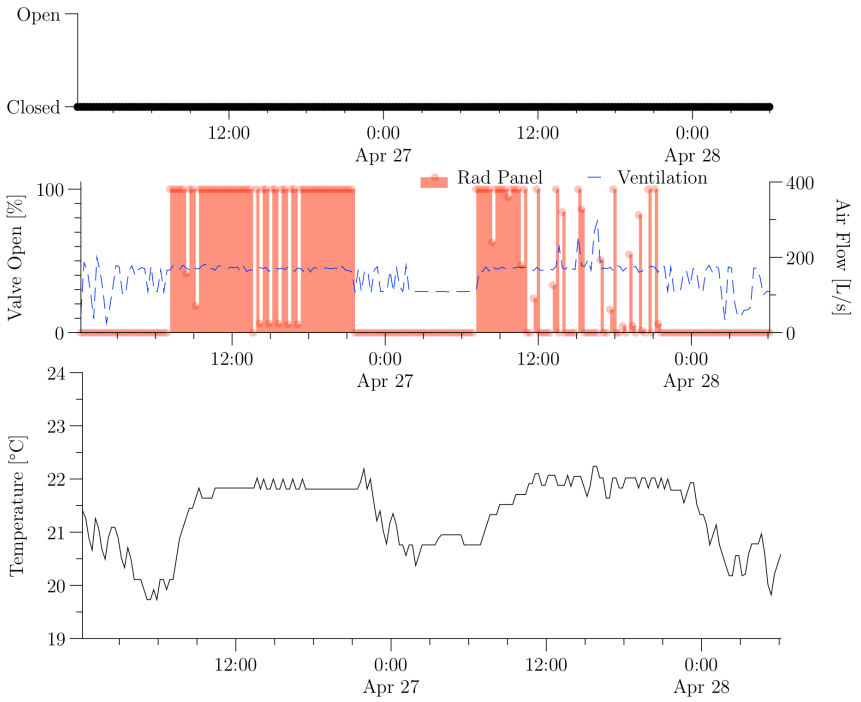

Figure 36: Sample office results.

The demonstration facility so far has provided a number of insights, both expected and unexpected, but still remains an on-going investigation. The original goal of being able to remove the zone from the existing BAS was a success, as was the implementation of an MPC strategy. The idea of using the neighbouring office spaces however is more challenging then originally anticipated because of their current control setup. The potential of altering the controls in the Delta Controls Lab is possible but purposely making the design system to match performance is non-ideal.

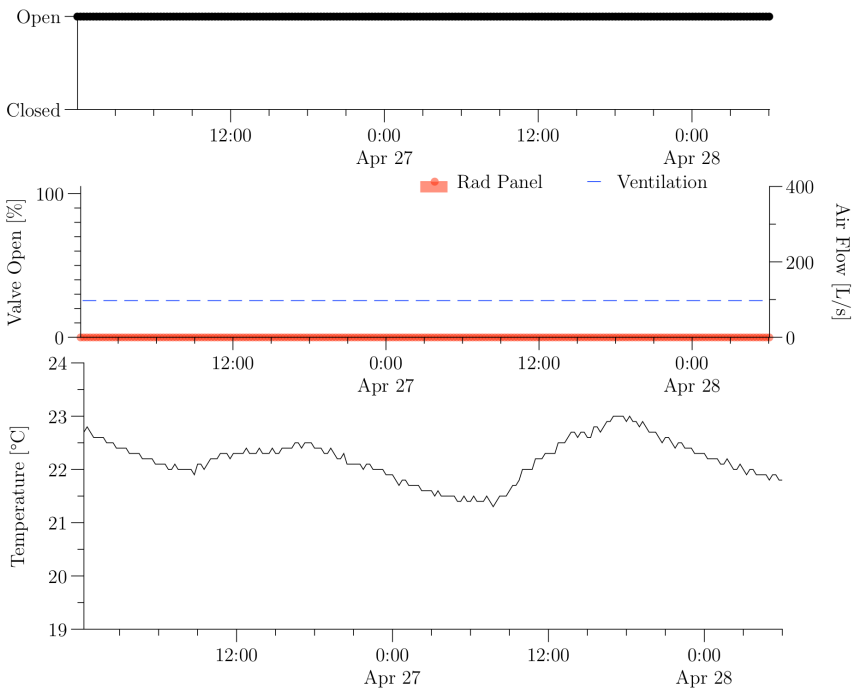

Figure 37: Delta Controls Lab results.

Chapter 6

Discussion

The combination of simulation work and brief demonstrative opportunity allowed for exploration both of the theoretical and practical aspects of a MPC-based shading controls. Based on these results and insights, discussion on the overall feasibility of MPC of blinds could occur.

6.1 Model-Based Control of Blinds Feasibility

Implementation of an MPC strategy for shading automation (or other HVAC control) systems are a viable solution to the increased automation of a building based off of both past and current simulation studies. Yet implementation in physical system remains infrequent and highly specialized. Part of the hesitation in the implementation of such strategies comes from the design of many of the applied approaches in the past. They have often relied on either full BPS constructions or high-order RC models that required detailed knowledge of the construction [17–22]. This approach is acceptable to the researcher but not for the industry personnel who is faced with time limitations during commissioning and who must consider the maintainability of a design for the life of the system. This facilitates the need for recursive methods that

are able to reduce the burden on operators and better utilize the capabilities of most BAS. Though identified as an effective method by past research [40,41] little has been done to address the implementation challenges into industrial applications by relying heavily on proprietary software such as MATLAB [42, 43]. Even in the attempts of this research, which were designed with application into the code of an existing BAS or simulation program explicitly sought, implementation was challenging and needed to be scaled back. The EMS of EnergyPlus is limited in many aspects, particularly the limiting of program lines to only 100 characters and the limiting of programs to only 120 lines. This coupled with a lack of array handling and lack of a robust compiling error-handler makes the implementation of any relatively large controls needlessly difficult. If it is not feasible to even create these controls in a simulated environment in which time and system operation are not as critical how can it be expected of operators of a physical BAS. During the implementation of the controls into the room controller, challenges were faced both in the hardware and software. Physically the devices ran into difficulty both in internal storage capacity and the processing of so much data. This resulted in the slowing down of refresh rates and functional speeds. In the software, the system was found to advertise functionality (such as data arrays) that were not reliable in execution. The end product in terms of developed control was found to be 10 to 20 times larger than the existing BAS code. These sorts of encountered problems were never mentioned by the researchers who actually performed physical installations, which is most likely a result of very little implementation that did not use custom control setups.

The exploration of how implementation could be performed was not considered in any of the literature, even in the studies where experimental runs of a physical situation were performed [21,30,31]. As more 'learning' algorithms become available in consumer goods (e.g., Nest Thermostats) there undoubtedly will be an increased

push for new recursive methods and the beginning of more accessible options particularly in this age of knowledge dissemination. One potential implementation strategy could take lessons from the architecture of current systems both in buildings and numerical software. As was found in the existing BAS of the Canal Building, advanced functionality (e.g., PID controllers) are embedded as predefined functions within the native language (GCL+). It is then highly conceivable that any recursive parameter estimation technique could be set up as a function in a similar fashion. This would remove a substantial portion of the learning curve to the designers and commissioners while still providing the functionality. The maintenance and innovation of these methods would be performed by the larger control companies who are already active in research and development. A similar built-in functionality could be applied to the modelling of a system at the zone level or room level for use as an MPC controller. If the EnKF was implemented in its general form its training abilities could be used by multiple different systems including setpoint learning, scheduling or HVAC controls.

The largest issue with the widespread application of the predictive, or even automated, shading would be the sourcing of the required motor for retrofits or the inclusion as part of a shading system purchase. From the experience gathered here it was found very few manufacturers are producing motors for shading applications. In many cases the motors that are designed are for the simple "open or close" situation and not the stepped motor response, which could have generated a more robust control option from a daylighting and occupant visual comfort aspect. In the implementation of automated shades in the New York Times Headquarters, Lee *et al.* [66] noted the same difficulty in sourcing of these devices, with most available products catering to niche market applications. Many of the retrofit applications of shades are in fact not in the domain of industrial products at all and are more in the realm of the hobbyist looking for a project. This situation does illustrate the possibility of how

this system could be made modular; separated from the central BAS and operating by its own governed controller embedded within the shade assembly. It would however be difficult to calibrate for the same thermal control benefits that the fully integrated system would be able to achieve. The addition of the motor to the shades would add complexity to the façade design as the motor cost per shade is not insignificant at the moment, so a cost-benefit analysis would need to occur for the project.

The commissioning of this system was not without its 'workarounds, which in a full-scale system could be revised. The largest of these was the reliance on the photodiodes to translate the solar energy flux into the room which is inefficient and potentially difficult to calibrate. Even with extensive calibration of a reactive system, as was completed in the New York Times Building, correlations became invalid not by the changes to the building or its envelope but by the construction of the buildings around the office tower [66]. This highlights how calibration would be susceptible to becoming uncalibrated relatively easily even before the consideration of the changing of surface materials, or reorganization of furniture. Fortunately, access to pyranometers here meant that the measured flux could be correlated to ceiling measurements, however these values are highly influenced to the light availability during calibration. The correlation used here, though deemed acceptable, still had a high degree of inaccuracy in capturing the relationship. A more suitable approach would be the inclusion of pyranometers as part of the BAS on the interior side of the glazing. This was not accomplished because of the lack of compatibility between the sensor and the controller but could be rectified by hardware companies if so insisted by demand. This would have reduced the need of on-site calibration (an expensive proposition in industry) and provided more reliable results. This device (depending on the complexity of the design of the building) would not be required in all zones and could be installed singularly for each orientation. Expanding on the idea of adapting controls,

these relations could be continually be updated recursively by software in a similar method to other setpoint values by the system.

6.1.1 Economic Feasibility

An aspect of any proposed strategy is of course the economic benefit of the system. The relative cost over a standard shading system in an office would only be the motor installation. The hardware costs of the Somfy devices used in the Delta Controls Lab were $235 per device, which ideally could cover up to a 10 foot span and a $90 wireless receiver to connect to an existing BAS. The use of wired alternatives, if considered early enough in the design phase, would also be possible and potentially a better alternative. The scope of the acquired data for the demonstrative setup would not allow for the cost savings to be calculated so the calculations come from the simulation contributions. From the *shoebox models* physical dimensions a single motor could be utilized by a window twice as wide. The sunken costs of the instillation compared to the cumulative savings are shown in Fig. 38. Based on this, the payback period, when not considering savings in capital costs on the HVAC, for this system would have been just over 6 years. This cost is highly dependent on the orientation, design of passive shading elements and material parameters. As such the implementation of these controls would have a higher payback period on all other orientations. Compared to other payback periods on energy retrofits of Canadian office buildings, as reported by Chidiac *et al.* [67] lighting energy reduction retrofits had payback periods of 5.8 to 7.5 years. Comparatively then, these values are competitive with other retrofits.

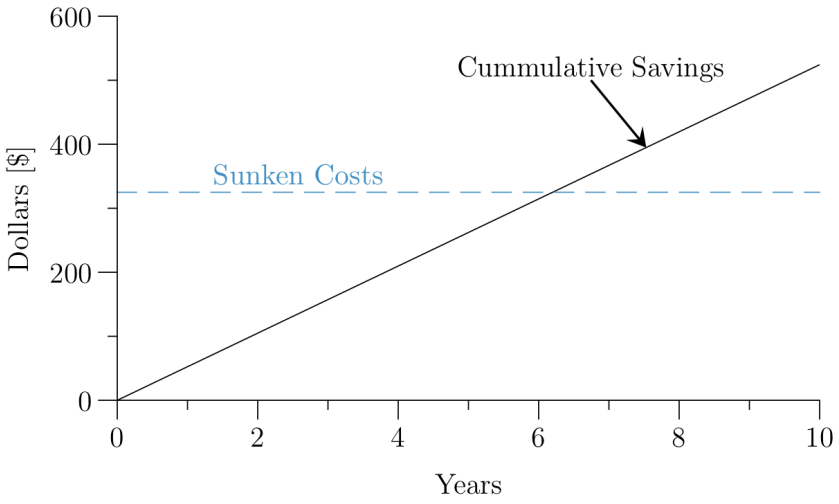

Figure 38: Simple payback period representation.

Chapter 7

Conclusions and Future Work

7.1 Conclusions

The study, design and development of a predictive, model-based shading control strategy were accomplished. The predictive shading controls were designed to utilize a building's thermal mass by predicting the building's thermal response to a number of factors over a prediction-time-horizon and automated shade positions in a way that reduces the costs (both electrical and monetary) of the building's operation.

A numerical investigation was accomplished using a *shoebox model* (i.e., a single-zone office space) that solved challenges including recursive parameter estimation techniques and implementation and compared strategies. Low-order control models were trained using the Bayesian method of an EnKF and their performance were compared to a brute-force global search optimization. In comparing strategies the first and second-order models both resulted in similar parameter estimates, both models were not without their implementation issues including lack of potential convergence when system perturbation were not large enough. Based on the comparisons it was found that a first-order RC model was actually able to outperform the second-order counterpart in a situation where limited system information was provided.

In the simulated office space an automated reactive strategy was compared to that of an implemented MPC strategy. Two different methods were attempted, one in which electricity use was minimized and one in which total utility costs were minimized. Both methods resulted in similar savings in electricity and cost. It was ultimately determined that using cost gave a higher savings but that the amount of electricity used by the system did not change. Electricity savings for heating and cooling were found to be 42% and 26% respectively in a system that controlled for only thermal benefits. If an automated lighting system was explored that allowed the lights to be turned off when shades were closed with high solar gains, the heating, cooling and lighting savings were reduced by 12%, 49% and 54%. Overall this led to a 35% reduction in total energy use. Financially, this system was calculated to have a payback period of at least 6 years in ideal circumstances.

Finally, a demonstration facility was constructed within the Delta Controls Lab and a brief study was conducted. Along with automated shades, a number of sensors and controllers were set up in order to recreate a small-scale BAS that could actively be tested. A modified predictive scheme was installed that addressed a number of the complications and shortcomings discovered during its commissioning. In terms of thermal comfort, the controls were able to keep the building zone in a thermal comfort range while reducing the space's reliance on the conditioning system. The system was able to do this while maintaining a level of visual comfort during occupied hours. During non-occupied weekends, the system was found to perform as expected and drastically reduce the energy use as compared to an identical office with manual shades and a control setup from the existing BAS of the building. A majority of the savings was not from the active control of shading devices and were a result of a more robust set of setpoints and control strategies for the ventilation and radiant panels then existed in the building's existing BAS. This result illustrates one of the main

problems with current building's and how they are controlled.

7.2 Recommendations for Future Work

The architectural trend of transparent building envelopes has become mainstream, but how to manage the increased levels of solar gains in ways that are not only beneficial to the building's operation but create an acceptable environment to the building's occupants is becoming a critical issue. A considerable amount of effort should be placed into the scalability and effectiveness of any solution that seeks to address these issues and relieve the considerable amount of reliance on so-called "active occupants". As the method developed has shown promise, it should be given more time to get more meaningful results. If possible a better set of measurements in terms of energy use and occupant satisfaction in the both the Delta Controls Lab and the existing neighbouring offices would allow for more energy quantifications to be performed. There would be considerable benefit in the ability to have the neighbouring systems adjusted to address many of the anomalies encountered during its observation.

With automated shades being so pivotal to visual and thermal comfort of the occupants the system must be adaptable to the occupant's request and desire for overrides. As such these occupant adjustments need to be tracked by the system and, if possible, learned from to create an environment that continually evolves with occupant desire and predicts actions that minimize the need for occupant interactions. Introductory work on this concept has already been developed by Gunay *et al.* [68] and would be easily included with what would work out to only be a software update to the BAS. Another element of the controller on the software side which was not included so far was a recursive estimation of the thermal parameters by the installed

building controller. Based on the experiences here many of the ideas developed and explored numerically were unable to be implemented in industry standard equipment. A more scalable approach relying on more standard operations should be tested.

Finally an assortment of environments should be investigated both in simulation and with the outfitting of MPC-based shades. With regard to simulation, only one climate zone was used in this work. Differing climates could be accommodated with little effort and could benefit more or less by this strategy. Similarly, only one style of shading technology was implemented with only open and closed control options. Alternative shading styles such as venetian shades or the ability to close a roller blind only half way would add control options particularly in terms of occupant comfort considerations. In terms of the physical implementation, only so much can be learned from a single office space that is occupied by a group of students who are more informed and complacent to building research. A project of this scale would provide valuable insights into the occupant interaction but also the problems associated with a retrofit project that could come with various layouts, designs, orientations and currently installed resources.

List of References

[1] NRCan, "Energy use data handbook," 2010.

[2] T. Kuhn, C. Bühler, and W. Platzer, "Evaluation of overheating protection with sun-shading systems," *Solar Energy*, vol. 69, Supplement 6, no. 0, pp. 59–74, 2001.

[3] W. O'Brien, K. Kapsis, and A. Athienitis, "Manually-operated window shade patterns in office buildings: A critical review," *Building and Environment*, vol. 60, no. 0, pp. 319–338, 2013.

[4] A. Leaman and B. Bordass, "Assessing building performance in use 4: the probe occupant surveys and their implications," *Building Research & Information*, vol. 29, no. 2, pp. 129–143, 2001.

[5] G. S. Brager, G. Paliaga, and R. De Dear, "Operable windows, personal control, and occupant comfort.," *Ashrae Transactions*, vol. 110, no. 2, 2004.

[6] K. V. D. Wymelenberg, "Patterns of occupant interaction with window blinds: A literature review," *Energy and Buildings*, vol. 51, no. 0, pp. 165 – 176, 2012.

[7] E. Lee, D. DiBartolomeo, and S. Selkowitz, "Thermal and daylighting performance of an automated venetian blind and lighting system in a full-scale private office," *Energy and buildings*, vol. 29, no. 1, pp. 47–63, 1998.

[8] A. Tzempelikos and A. Athienitis, "The impact of shading design and control on building cooling and lighting demand," *Solar Energy*, vol. 81, no. 3, pp. 369–382, 2007.

[9] M. Velds, "User acceptance studies to evaluate discomfort glare in daylit rooms," *Solar Energy*, vol. 73, no. 2, pp. 95–103, 2002.

[10] C. Reinhart and K. Voss, "Monitoring manual control of electric lighting and blinds," *Lighting Research and Technology*, vol. 35, no. 3, pp. 243–258, 2003.

[11] Y. Sutter, D. Dumortier, and M. Fontoynont, "The use of shading systems in vdu task offices: a pilot study," *Energy and Buildings*, vol. 38, pp. 780–789, 2006.

[12] K. Konis, "Evaluating daylighting effectiveness and occupant visual comfort in a side-lit open-plan office building in san francisco, california," *Building and Environment*, vol. 59, no. 0, pp. 662 – 677, 2013.

[13] M. Skelly and M. Wilkinson, "The evolution of interactive facades: Improving automated blind control," *Whole Life Performance of Facades*, pp. 129–142, 2001.

[14] P. May-Ostendorp, G. Henze, B. Rajagopalan, and C. Corbin, "Extraction of supervisory building control rules from model predictive control of windows in a mixed mode building," *Journal of Building Performance Simulation*, vol. 6, no. 3, pp. 199–219, 2012.

[15] E. Vrettos, K. Lai, F. Oldewurtel, and G. Andersson, "Predictive control of buildings for demand response with dynamic day-ahead and real-time prices," in *Control Conference (ECC), 2013 European*, pp. 2527–2534, July 2013.

[16] N. Motegi, M. A. Piette, D. S. Watson, S. Kiliccote, and P. Xu, "Introduction to commercial building control strategies and techniques for demand response," *Lawrence Berkeley National Laboratory LBNL-59975*, 2007.

[17] E. S. Lee and S. E. Selkowitz, "The design and evaluation of integrated envelope and lighting control strategies for commercial buildings," vol. 101(1) of *ASHRAE Transactions*, 06/01/1994 1994.

[18] P. May-Ostendorp, G. Henze, C. Corbin, B. Rajagopalan, and C. Felsmann, "Model-predictive control of mixed-mode buildings with rule extraction," *Building and Environment*, vol. 46, no. 2, pp. 428–437, 2011.

[19] A. Mahdavi and C. Pröglhöf, "A model-based approach to natural ventilation," *Building and Environment*, vol. 43, no. 4, pp. 620–627, 2008.

[20] A. Mahdavi, "Predictive simulation-based lighting and shading systems control in buildings," *Building Simulation*, vol. 1, no. 1, pp. 25–35, 2008.

[21] A. Mahdavi, M. Schuss, G. Suter, S. Metzger, S. Camara, and S. Dervishi, "Recent advances in simulation-powered building systems control," 2009.

[22] C. Corbin, G. Henze, and P. May-Ostendorp, "A model predictive control optimization environment for real-time commercial building application," *Journal of Building Performance Simulation*, vol. 6, no. 3, pp. 159–174, 2012.

[23] D. Gyalistras and M. Gwerder, "Use of weather and occupancy forecasts for optimal building climate control (opticontrol): Two years progress report," *Terrestrial Systems Ecology ETH Zurich, Switzerland and Building Technologies Division, Siemens Switzerland Ltd., Zug, Switzerland*, 2010.

[24] F. Oldewurtel, A. Parisio, C. Jones, M. Morari, D. Gyalistras, M. Gwerder, V. Stauch, B. Lehmann, and K. Wirth, "Energy efficient building climate control using stochastic model predictive control and weather predictions," in *American Control Conference (ACC), 2010*, pp. 5100–5105, 2010.

[25] F. Oldewurtel, A. Ulbig, A. Parisio, G. Andersson, and M. Morari, "Reducing peak electricity demand in building climate control using real-time pricing and model predictive control," in *Decision and Control (CDC), 2010 49th IEEE Conference on*, pp. 1927–1932, 2010.

[26] F. Oldewurtel, A. Parisio, C. Jones, D. Gyalistras, M. Gwerder, V. Stauch, B. Lehmann, and M. Morari, "Use of model predictive control and weather forecasts for energy efficient building climate control," *Energy and Buildings*, vol. 45, no. 0, pp. 15–27, 2012.

[27] V. Stauch, C. Hug, F. Schubiger, and P. Steiner, "Weather forecasts, observations and algorithms for building simulation and predictive control," *OptiControl report on the Contributions by MeteoSwiss*, 2010.

[28] M. Gwerder, D. Gyalistras, F. Oldewurtel, B. Lehmann, K. Wirth, V. Stauch, J. Tödtli, and C. J. Tödtli, "Potential assessment of rule-based control for integrated room automation," in *10th REHVA World Congress Clima*, pp. 9–12, 2010.

[29] M. Gwerder and J. Tödtli, "Predictive control for integrated room automation," in *8th REHVA World Congress Clima*, 2005.

[30] Y. Ma, F. Borrelli, B. Hencey, A. Packard, and S. Bortoff, "Model predictive control of thermal energy storage in buiding cooling systems," in *Decision and*

Control, 2009 held jointly with the 2009 28th Chinese Control Conference. CDC/CCC 2009. Proceedings of the 48th IEEE Conference on, pp. 392–397, 2009.

[31] Y. Ma, F. Borrelli, B. Hencey, B. Coffey, S. Bengea, and P. Haves, "Model predictive control for the operation of building cooling systems," *Control Systems Technology, IEEE Transactions on*, vol. 20, no. 3, pp. 796–803, 2012.

[32] M. Kummert, P. André, and J. Nicolas, "Optimal heating control in a passive solar commercial building," *Solar Energy*, vol. 69, Supplement 6, no. 0, pp. 103–116, 2001.

[33] M. Kummert, P. André, and A. Argiriou, "Comparing control strategies using experimental and simulation results: Methodology and application to heating control of passive solar buildings," *HVAC&R Research*, vol. 12, no. sup1, pp. 715–737, 2006.

[34] M. Kummert and P. André, "Simulation of a model-based optimal controller for heating systems under realistic hypothesis," 2005.

[35] P. Fanger, *Thermal Comfort Analysis and Applications in Environmental Engineering*. MacGraw Hill, 1972.

[36] P. Radecki and B. M. Hencey, "Online thermal estimation, control, and self-excitation of buildings," in *Proceedings of IEEE Conference on Decision and Control, Florence, IT*, (Firenze, Italy), IEEE, Dec. 2013.

[37] T. Y. Chen and A. K. Athienitis, "Investigation of practical issues in building thermal parameter estimation," *Building and Environment*, vol. 38, no. 8, pp. 1027–1038, 2003.

[38] T. Dewson, B. Day, and A. Irving, "Least squares parameter estimation of a reduced order thermal model of an experimental building," *Building and Environment*, vol. 28, no. 2, pp. 127 – 137, 1993. Special Issue Thermal Experiments in Simplified Buildings.

[39] J. Braun and N. Chaturvedi, "An inverse gray-box model for transient building load prediction," *HVAC&R Research*, vol. 8, no. 1, pp. 73–99, 2002.

[40] S. Fux, A. Ashouri, M. Benz, and L. Guzzella, "EKF based self-adaptive thermal model for a passive house," *Energy and Buildings*, vol. 68, Part C, no. 0, pp. 811 – 817, 2014.

[41] P. Radecki and B. Hencey, "Online building thermal parameter estimation via Unscented Kalman Filtering," in *American Control Conference (ACC), 2012*, pp. 3056–3062, 2012.

[42] J. Candanedo and A. Athienitis, "Simplified linear models for predictive control of advanced solar homes with passive and active thermal storage," in *First High Performance Building Conference*, Purdue University, July 2010.

[43] J. A. Candanedo, V. R. Dehkordi, and P. Lopez, "A control-oriented simplified building modelling strategy," in *13th Conference of international Building Performance Simulation Association*.

[44] "Getting started with energyplus - basic concepts manual," tech. rep., Lawrence Berkeley National Laboratory, 2013.

[45] "ASHRAE 90.1-2010 standard-energy standard for buildings except low-rise residential buildings."

[46] G. Newsham, "Manual control of window blinds and electric lighting: Implications for comfort and energy consumption," *Indoor and Built Environment*, vol. 3, no. 3, pp. 135–144, 1994.

[47] C. Reinhart, "Lightswitch-2002: a model for manual and automated control of electric lighting and blinds," *Solar Energy*, vol. 77, no. 1, pp. 15–28, 2004.

[48] B. Huchuk, W. O'Brien, and C. A. Cruickshank, "Preliminary results of model predictive control of shading systems (wip)," in *Proceedings of the Symposium on Simulation for Architecture & Urban Design*, p. 29, Society for Computer Simulation International, 2013.

[49] S. Wang and X. Xu, "Simplified building model for transient thermal performance estimation using ga-based parameter identification," *International Journal of Thermal Sciences*, vol. 45, no. 4, pp. 419 – 432, 2006.

[50] G. Hudson and C. Underwood, "A simple building modelling procedure for matlab/simulink," in *International Building Performance and Simulation Conference, Kyoto*, 1999.

[51] M. Gouda, S. Danaher, and C. Underwood, "Building thermal model reduction using nonlinear constrained optimization," *Building and Environment*, vol. 37, no. 12, pp. 1255 – 1265, 2002.

[52] T. R. Nielsen, "Simple tool to evaluate energy demand and indoor environment in the early stages of building design," *Solar Energy*, vol. 78, no. 1, pp. 73 – 83, 2005.

[53] J. Clarke, *Energy simulation in building design*. Routledge, 2001.

[54] G. Evensen, "The ensemble kalman filter: theoretical formulation and practical implementation," *Ocean Dynamics*, vol. 53, no. 4, pp. 343–367, 2003.

[55] G. Evensen, "Sequential data assimilation with a nonlinear quasi-geostrophic model using monte carlo methods to forecast error statistics," *Journal of Geophysical Research: Oceans*, vol. 99, no. C5, pp. 10143–10162, 1994.

[56] Y. He, X. Liu, C. Zhang, and Z. Chen, "A new model for state-of-charge (soc) estimation for high-power li-ion batteries," *Applied Energy*, vol. 101, no. 0, pp. 808 – 814, 2013. Sustainable Development of Energy, Water and Environment Systems.

[57] J. Ching, J. L. Beck, and K. A. Porter, "Bayesian state and parameter estimation of uncertain dynamical systems," *Probabilistic Engineering Mechanics*, vol. 21, no. 1, pp. 81 – 96, 2006.

[58] R. Kalman, "A new approach to linear filtering and prediction problems," *Journal of basic Engineering*, vol. 82, no. 1, pp. 35–45, 1960.

[59] J. Mandel, "A brief tutorial on the ensemble kalman filter," Tech. Rep. 242, University of Colorado at Denver and Health Sciences Center, February 2007.

[60] G. Evensen, *Data assimilation: the ensemble Kalman filter*. Springer, 2009.

[61] R. Kramer, "From castle to binary code.," 2012.

[62] H. Gunay, W. O'Brien, I. Beausoleil-Morrison, B. Huchuk, M. Palmer, J. Fletcher, and A. Pavlovski, "The effect of input uncertainty in model-based predictive control," in *Proceedings of eSim, Ottawa, Ontario*, 2014.

[63] Hydro One, "Electricity prices." online.

[64] ASHRAE, "55: Thermal environmental conditions for human occupancy," *American Society of Heating, Refrigerating and Air-Conditioning Engineers, Atlanta*, 2010.

[65] F. Haldi and D. Robinson, "Adaptive actions on shading devices in response to local visual stimuli," *Journal of Building Performance Simulation*, vol. 3, no. 2, pp. 135–153, 2010.

[66] E. Lee, L. Fernandes, B. Coffey, A. McNeil, R. Clear, T. Webster, F. Bauman, D. Dickerhoff, D. Heinzerling, and T. Hoyt, "A post-occupancy monitored evaluation of the dimmable lighting, automated shading, and underfloor air distribution system in the new york times building," 2013.

[67] S. Chidiac, E. Catania, E. Morofsky, and S. Foo, "A screening methodology for implementing cost effective energy retrofit measures in canadian office buildings," *Energy and Buildings*, vol. 43, no. 2–3, pp. 614 – 620, 2011.

[68] H. Gunay, W. O'Brien, I. Beausoleil-Morrison, and B. Huchuk, "On adaptive occupant-learning window blind and lighting controls," *Building Research and Information*, pp. 1–18, April 2014.

[69] Z. Sen, *Solar energy fundamentals and modeling techniques: atmosphere, environment, climate change and renewable energy*. Springer, 2008.

[70] R. Leslie, "Capturing the daylight dividend in buildings: why and how?," *Building and Environment*, vol. 38, no. 2, pp. 381–385, 2003.

[71] C. Reinhart, J. Mardaljevic, and Z. Rogers, "Dynamic daylight performance metrics for sustainable building design," *Leukos*, vol. 3, no. 1, pp. 1–25, 2006.

[72] C. Reinhart and A. Fitz, "Findings from a survey on the current use of daylight simulations in building design," *Energy and Buildings*, vol. 38, no. 7, pp. 824–835, 2006.

[73] P. Moon and D. Spencer, "Illumination from a non-uniform sky," *Illuminating Engineering*, vol. 37, no. 10, pp. 707–726, 1942.

[74] A. Nabil and J. Mardaljevic, "Useful daylight illuminance: a new paradigm for assessing daylight in buildings," *Lighting Research and Technology*, vol. 37, no. 1, pp. 41–57, 2005.

[75] C. Reinhart and O. Walkenhorst, "Validation of dynamic radiance-based daylight simulations for a test office with external blinds," *Energy and Buildings*, vol. 33, no. 7, pp. 683–697, 2001.

[76] A. Tenner, S. Begemann, and G. Van den Beld, "Acceptance and preference of illuminances in offices," *Proceedings Lux Europa (Amsterdam, the Netherlands)*, 1997.

[77] A. Nabil and J. Mardaljevic, "Useful daylight illuminances: A replacement for daylight factors," *Energy and Buildings*, vol. 38, no. 7, pp. 905–913, 2006.

[78] M. Rea, *The IESNA lighting handbook: reference and application*. 2000.

[79] W. Osterhaus and I. Bailey, "Large area glare sources and their effect on visual discomfort and visual performance at computer workstations," in *Industry Applications Society Annual Meeting, 1992., Conference Record of the 1992 IEEE*, pp. 1825–1829 vol.2, 1992.

[80] W. Osterhaus, "Discomfort glare assessment and prevention for daylight applications in office environments," *Solar Energy*, vol. 79, no. 2, pp. 140–158, 2005.

[81] R. Hopkinson and R. Bradley, "A study of glare from very large sources," *Illuminating Engineering*, vol. 55, no. 5, pp. 288–294, 1960.

[82] P. Chauvel, J. Collins, R. Dogniaux, and J. Longmore, "Glare from windows: current views of the problem," *Lighting Research and Technology*, vol. 14, no. 1, pp. 31–46, 1982.

[83] A. Nazzal, "A new daylight glare evaluation method: Introduction of the monitoring protocol and calculation method," *Energy and Buildings*, vol. 33, no. 3, pp. 257–265, 2001.

[84] K. Fisekis, M. Davies, M. Kolokotroni, and P. Langford, "Prediction of discomfort glare from windows," *Lighting Research and Technology*, vol. 35, no. 4, pp. 360–369, 2003.

[85] H. Einhorn, "Discomfort glare: a formula to bridge differences," *Lighting Research and Technology*, vol. 11, no. 2, pp. 90–94, 1979.

[86] I. C. on Illumination, *Discomfort Glare in Interior Lighting*. CIE technical report, Commission Internationale de l'Éclairage, 1995.

[87] J. Jakubiec and C. Reinhart, "The 'adaptive zone' – a concept for assessing discomfort glare throughout daylit spaces," *Lighting Research and Technology*, vol. 44, no. 2, pp. 149–170, 2012.

[88] S. Guth, "A method for the evaluation of discomfort glare," *Illuminating Engineering*, vol. 58, no. 5, pp. 351–364, 1963.

[89] N. Ruck, "International energy agency's solar heating and cooling task 31,'daylighting buildings in the 21st century'," *Energy and buildings*, vol. 38, no. 7, pp. 718–720, 2006.

[90] J. Wienold and J. Christoffersen, "Evaluation methods and development of a new glare prediction model for daylight environments with the use of ccd cameras," *Energy and Buildings*, vol. 38, no. 7, pp. 743–757, 2006.

[91] J. Wienold, "Dynamic daylight glare evaluation," in *Proceedings of Building Simulation*, pp. 944–951, 2009.

[92] "2009 ASHRAE Handbook - Fundamentals (SI Edition)," 2009.

[93] S. Selkowitz, "Integrating advanced facades into high performance buildings," 2001.

Appendix A

Daylighting Fundamentals

A.1 Daylight

The most fundamental aspect to the concept of solar control and daylighting is the source of all natural light on planet — the sun. The sun admits a broad-spectrum of electromagnetic (EM) radiationThe source of the most of the solar radiation is the sun's photosphere. The extraterrestrial irradiance (i.e solar radiation at the top of the earth's atmosphere) is approximated as blackbody radiation at 5800K. The peak of the solar spectrum occurs between wavelengths of 380 - 770 nm, which happens to correspond to visible range of the human eye [69].

As the sun's radiation passes through the atmosphere certain wavelengths are absorbed and attenuated (not all equally) by various components of the atmosphere. As a result the power of the solar radiation drops from an average value of
1360 $W \cdot m^{-2}$ at the surface of the atmosphere down to levels at sea level varying from 80 $W \cdot m^{-2}$ to 1200 $W \cdot m^{-2}$ during the solar noon; based on variables including latitude, season and solar conditions.

Sunlight is more efficient in terms of luminous efficacy, then most commercial artificial lighting used in commercial buildings which provides a broad electromagnetic

spectrum which creates a more dynamic interior space which promotes better human health and performance [70], too much of a good thing however can be detrimental and can lead to situations of glare. It can not be forgotten as well, that light is still in fact a radiant energy and energy outside of the visible spectrum still exists and will heat the interior environment which can be undesirable in buildings.

A.2 Daylight Performance Metrics

Daylight, though an integral part of a building environment, has no standard performance metric. With so many different shading, control and interior options it is important to understand what happens within a building space. Unfortunately, unlike other building environment metrics, daylight is a "notoriously difficult" [71] building performance aspect to quantify. With the increase of computation power and simulation, more of the daylight analysis is being conducted through simulation, and with it more parties are becoming involved in the design of the building quantify daylighting as something included in the design process [72].

Historically used, the Daylight Factor (DF) is defined as the ratio of the internal illuminance at a point in a building to the unshaded, external horizontal illuminance under a CIE (International Commission on Illumination) overcast sky [73]. Never intended to be a measure of good daylighting design, it was instead intended to be a minimum legal lighting requirement [71]. Even so it remains the most widely used performance measure of quantitative daylighting measure [72, 74] Daylight factors continued usage is a result of its responsiveness to a buildings geometry, surrounding landscape and buildings, and surface properties. Further the same features that often are associated with good daylighting correspond to high DF values. However, the DF value takes the approach that the more light the better, which often is not the

case. Other drawbacks include, that its sky model uses worst case sky conditions, and that the DF value is the same for all façade orientation and building locations which removes its ability to help develop glare prevention strategies on multiple façades.

Reihnart and Walkenhorst [75], were the most recent to update the definition of Daylight Autonomy (DA) to be the fraction of a considered time interval which a minimum illuminance level can be maintained by daylight alone at a specific point. Typically the time interval in question are the hours per year when a workplane is occupied. The required minimum illuminance level can range from 150 [46] to more then 1000 lux [76] based on legal requirements or user preferences. When investigating workplane illuminance, several points on the centre line of a room from the façade to the back wall are used for measurements.

Useful Daylight Illuminance (UDI) was developed by Nabil and Maradalievic [74] and was designed to be a more robust alternative for daylight factors. Unlike daylight factors, UDI is a climate-based analysis which utilizes realistic, time-varying sky and sun conditions to predict hourly levels of absolute daylight illuminance [77]. Instead of calculating the meeting of a threshold value of illuminance, UDI is the percentage of occupied hours per year where daylight levels are useful. Useful is defined as any illuminance falling within the range of 100-2000 lux, while lower then 100 lux or larger then 2000 lux are considered not to be useful as they have found to be insufficient as a sole source of illumination or likely to produce visual or thermal discomfort, or both [77] respectively. When investigating workplane illuminance, it is investigated for several points on the centre line of a room from the façade to the back wall, just like DA.

These daylighting metrics are looked at as a signs of a well designed building in terms of daylighting, and are the most widespread by professionals investigating daylighting topics [72]. The drawback of allowing so much light into a space is the

potential for visual discomfort and cause glare - a topic none of these metrics address.

A.3 Visual Comfort

Visual comfort is perhaps the most important aspect of the proper daylighting of any space. Often a blind system, automated or not is fundamental if a daylit space is too meet the demands of a user in a comfort respect. Heuristic lighting set points are designed to be conservative and avoid glare, but more importantly the possibility of complaints. Lighting standards typically require an office workplane illuminance of at least 500 lux where paper-based work is carried out. Lower workplace illuminaces should be used when a computer and visual display unit (VDU) are used [78], but conditions should never go below 100 lux as it is deemed too dark while anything over 2000 lux is considered likely to produce glare [77].

Glare is attempted to be avoided when utilizing daylight, but what glare is exactly is difficult to quantify and therefore difficult to avoid. In the Lighting Handbook of the Illuminating Engineering Society of North America, glare is defined as the sensation produced by luminance within the visual field that is sufficiently greater then the luminance to which the eyes are adapted to cause annoyance, discomfort or loss in in visual performance and visibility [78].

Glare is divided into two main categories - disability and discomfort. Disability glare is physiological condition where stray light in the eye reduces visibility and visual performance from a reduction of contrast. For example, direct sunlight or reflections from a bright window off a shiny surface or a VDU. Discomfort glare alternatively is a psychological condition, and therefore is highly subjective. It ultimately does not necessarily reduces visual performance or visibility but does provide annoyance from high contrast between luminous sources and room surfaces. Discomfort glare is

highly dependent on the angular displacement of the source from the observers line of sight and the size of the source of glare [79].

Occupants tend to have different reactions to each type of glare. When disability glare occurs, occupants tend to adjust their position or utilize a shading device [80]. Discomfort glare can occur with no change to the work performance of the occupant but headaches and eyestrain might develop due to continuous adaption of the eyes to the highly contrasting lighting conditions. Discomfort glare is the more common issue within a building, and being so subjective, is where glare metrics and quantifications have been attempted to be applied.

A.3.1 Glare Quantification

With the subjective nature of discomfort glare, attempts have had to be made to create metrics which predict the human response. Osterhaus [80] investigated the current state of these attempts and their predictive capabilities. The investigation concluded that the available methods are of limited practical use for daylight offices and that no method had been developed a unified model for both daylighting and electrical lighting. Major glare indices are the Daylight Glare Index (DGI), the CIE Glare Index (CGI), the Unified Glare Rating System (UGR), the Visual Comfort Probability (VCP) and Daylight Glare Probability (DGP).

The DGI (or Cornell Equation), Eqn. 22, was first developed by Hopkinson and Bradley [81] following research at the Building Research Station in England and at Cornell University. It was developed for quantifying discomfort glare from daylighting (the first discomfort glare index to not be developed for artificial lighting). Since the initial investigation, others have attempted to modify and build off the original model. Chauvel *et al.* [82] investigated how the values of glare discomfort changed for the different components composing daylight. Nazzal [83] revised the DGI and developed

the DGIN, derived a model that assessed the degree of visual discomfort based which could be implemented in RADIANCE, which provides luminance values. One of the major revelations from Nazzal and Chutarat was substituting average luminance, with background luminance. This adjustment was experimentally supported by the work of Fisekis *et al.* [84]. Despite its advances, evolution and widespread adoption, it still can lead to unreliable results with limitations coming from non-uniform glare sources and size of glare source [80].

The CGI, Eqn. 23, was adopted by the CIE following a tasked investigation by Einhorn to develop a compromising and standard glare calculating procedure [85]. The resulting equation took elements from existing knowledge and blended results and approaches used in different nations and researchers at the time. The formulation was acknowledged to be not be reliable in all circumstance and environments and was intended to be a starting point for more complete analysis with more field-work support and equation adjustments in the future [85].

The CIE proposed and implemented an updated to the CGI method in the form the UGR, Eqn. 24 [86] , which among other things addressed the inability of CGI to handle the additivity of glare source areas [84] and the difficulty in measuring direct illuminance [87]. The system was developed with data only from artificial light sources and restricts the angular source size to a range of solid angles. The approach is not recommended for discomfort glare from indirect lighting or non-uniform luminaries of large glare sources. It was intended to a be a more computationally-friendly alternative to the earlier CGI metric; but it has been found that the exact testing procedure and method for development is not clearly discussed [87].

The VCP, Eqn. 25, is a more complex version of the Guth discomfort glare ratio (DGR) [88] - a very early glare metric. The VCP is another strictly empirical model, which was defined by the Illuminating Engineering Society of North America

(IESNA). It is only valid in situations with standard sized, ceiling mounted artificial lighting instillation with uniform luminances. It is unable to deal with very small or very large glare sources; meaning it does not provide accurate results in spaces with daylighting sources.

The DGP metric, Eqn. 26 , was developed from SubTask A of the International Energy Agency's (IEA) Solar Heating and Cooling Task 31 in order to model the occupant's use of lighting and glare controls [89]. Research was conducted by Wienold and Christoffersen [90] on experiments in Germany and Holland in which responses from surveyed users were correlated to measurements of a CCD camera. The DGP works to replace other discomfort glare indices and takes into consideration glare sources as a result of focus on a work task and not direct viewing of the glare source. The relation ended up being a result of vertical eye illuminance, the glare source term of CIE glare index and some empirically derived constants. It seeks to calculate the probability that a person is disturbed by glare. Particularly novel compared to past methods is the ability to predict discomfort in bright scenes when visual contrast is not significant. Most notable is the implementation of this formula into the Evalglare a simulation engine based off of RADIANCE. Weinold was responsible for the development of a simplified daylight glare probability (DGPs) that only correlates glare to vertical illuminance [91], shown in Eqn. 26. This method is much easier to calculate using simulation results and is the approach used by OpenStudio when RADIANCE is used for glare calculations. The major limitation of this approach is the neglecting of any individual glare sources and for that reason can only be applied when there is no direct sun or specular reflections hitting the observers eyes [91].

$$DGI = 10 \cdot \log \left(0.478 \sum_i \frac{L_{s,i}^{1.6} \cdot \omega_{s,i}^{0.8}}{L_b + 0.07 \cdot \omega^{0.5} \cdot L_{s,i}} \right) \tag{22}$$

$$CGI = 8 \cdot \log\left(2 \cdot \frac{1 + \left(\frac{E_d}{500}\right)}{E_v} \sum_i \frac{L_{s,i}^2 \cdot \omega_{s,i}}{P_i^2}\right) \tag{23}$$

$$UGR = 8 \cdot \log\left(\frac{0.25}{L_b} \sum_i \frac{L_{s,i}^2 \cdot \omega_{s,i}}{P_i^2}\right) \tag{24}$$

$$VCP = \left[224.4 - 46.8 \cdot \log\left(\sum_i \left(\frac{0.5 \cdot L_{s,i} \cdot \left(20.4 \cdot \omega_{s,i} + 1.52 \cdot \omega_{s,i}^{0.2} - 0.075\right)}{P_i \cdot L_a^{0.44}}\right)^{-0.0914}\right)\right] + 50 \tag{25}$$

$$DGP = 5.87 \cdot 10^{-5} \cdot E_v + 0.092 \cdot \log\left(1 + \sum_i \frac{L_{s,i}^2 \cdot \omega_{s,i}}{P_i^2}\right) + 0.16 \tag{26}$$

$$DGPs = 6.22 \cdot 10^{-5} \cdot E_v + 0.184 \tag{27}$$

Each of these glare metrics works on its own scale and range of values as to what constitutes glare as Imperceptible, Perceptible, Disturbing and Intolerable. These threshold values are contained within Table 1. Similar in most values is that lower value pertain to lower glare; the only exception being VCP.

Table A.1: Glare indices values and thresholds.

Degree of Perceived Glare	DGP	DGI	UGR	VCP	CGI
Imperceptible	< 0.35	< 18	< 13	$80 - 100$	< 13
Perceptible	$0.35 - 0.40$	$18 - 24$	$13 - 22$	$60 - 90$	$13 - 22$
Disturbing	$0.40 - 0.45$	$24 - 31$	$22 - 28$	$40 - 60$	$22 - 28$
Intolerable	> 0.45	> 31	> 28	< 40	> 28

A.4 Fenestration

Fenestration is a general term referring to the windows, skylights and door systems of a building. These building components are relied upon to separate the interior and exterior environments and can effect the the building energy usage through four basic mechanisms: thermal heat transfer, air leakage, solar heat gain and daylighting [92]. As recent building trends have led to the design of highly transparent building faades [93], there has been increased research in the areas of optimizing fenestration using dynamic components to control the four major basic energy mechanisms. Though both conventional and innovative shading devices are being employed in commercial applications and seen as cutting-edge, a dynamic one (if even simple) that is able to provide both visual and thermal control to occupants under various environmental conditions can make substantial changes to building energy performance [8].

Appendix B

MATLAB Code

B.1 EnKF Training

The code contained in this section is an example of the EnKF code used for the training of the second-order model.

B.1.1 Initialization Program

```
clc
close all
clear all
%%------ Start Here ------%%

%designed to run Ensemble Kalman Filter (2R2C)

% Dec 7/2013
% Written By: Brent Huhcuk

% v3.2 - designed to split components with fractions upon surfaces and have
```

```
%        delayed starts and stops
%      - designed to use more available data
%      - Requires CSV to be in the same directory

%%====================== Retrieve Data ========================

%------Import EnergyPlus CSV data-------

%Import data and heading
results=importdata('Learning_newsol_noshade_inf_30min.csv',',',1);

results_headings=results.textdata(1,2:size(results.textdata,2));
data=results.data;
output_lines=size(data,1); %number of hours that simulation was run for

%Determine critical index values

index_zone_heat=find(strcmp(deblank(results_headings),...
'ASHRAE2014:Zone/Sys Sensible Heating Rate [W](TimeStep)')==1);

index_zone_cool=find(strcmp(deblank(results_headings),...
    'ASHRAE2014:Zone/Sys Sensible Cooling Rate [W](TimeStep)')==1);
index_Tamb=find(strcmp(deblank(results_headings),...
    'ASHRAE2014:Zone Outdoor Dry Bulb [C](TimeStep)')==1);

index_Window_HeatGain=find(strcmp(deblank(results_headings),...
    'SW:Surface Outside Face Solar Radiation Heat Gain Rate [W](TimeStep)'...
    )==1);

index_IndoorTemp=find(strcmp(deblank(results_headings),...
    'ASHRAE2014:Zone Mean Air Temperature [C](TimeStep)')==1);
```

```
index_People = find(strcmp(deblank(results_headings),...
    'ASHRAE2014:Zone People Number Of Occupants [](TimeStep)')==1);
index_Lights = find(strcmp(deblank(results_headings),...
    'ASHRAE2014:Zone Lights Electric Power [W](TimeStep)')==1);

index_HeatSP= find(strcmp(deblank(results_headings),...
    'ASHRAE2014:Zone/Sys Thermostat Heating Setpoint [C](TimeStep)')==1);
index_CoolSP= find(strcmp(deblank(results_headings),...
    'ASHRAE2014:Zone/Sys Thermostat Cooling Setpoint [C](TimeStep)')==1);

index_infgain = find(strcmp(deblank(results_headings),...
    'ASHRAE2014:Zone Infiltration Sensible Heat Gain [J](TimeStep)')==1);
index_infloss = find(strcmp(deblank(results_headings),...
    'ASHRAE2014:Zone Infiltration Sensible Heat Loss [J](TimeStep)')==1);

%Remove data
Load_Heat = data(:,index_zone_heat);
Load_Cool = data(:,index_zone_cool);
Qhvac = Load_Heat + Load_Cool*(-1);
Tamb_full = data(:,index_Tamb);
Qsol_full = data(:,index_Window_HeatGain)*1;
Tin_full = data(:,index_IndoorTemp);
Qpeople = data(:,index_People)*100;
Qlights = data(:,index_Lights);
HeatSP = data(:,index_HeatSP);
CoolSP = data(:,index_CoolSP);
Inf_gain = data(:,index_infgain)/(60*30);
Inf_loss = data(:,index_infloss)*(-1)/(60*30);

% Combine loads for single Qaux term
Qt_full = Qhvac + Qpeople + Qlights + Inf_gain + Inf_loss;
```

```
%%====================== Run EnKF ========================

%------- Initialize parameters --------
TSH = 2; % number of timesteps per hour
TSm = 30; % number of minutes in a timestep

N=2000; %number of ensembles
dt=60*TSm; %time-step

QsolFrac = 0.3;
QtFrac = 0.7;

timestart = 24*7*2*TSH + 0*TSH; %when training starts
timelength = 24*7*24*TSH; % how long to train data
trainingperiod = timestart + timelength; %how long the training occurs

%------- Data Prep --------
%Trim data to appropriate lengths **add a +1 to timestart

Tamb = Tamb_full(timestart:(trainingperiod + 24*TSH));
Qt = Qt_full(timestart:(trainingperiod + 24*TSH));
Qsol = Qsol_full(timestart:(trainingperiod + 24*TSH))*0.6;
Tin  = Tin_full(timestart:(trainingperiod + 24*TSH));

%------ Assign Initial Value Estimates ------

%Parameters to be estimated
Rw_mean =1.5*10^(-1);
Cw_mean =9.0*10^(4);
```

```
Ri_mean = 5.32*10^(-1);
Ci_mean =3.02*10^(3);

Tw_mean = 0;

gamma = 0.5; %Meausrement Error

%------- Create Inital Ensembles --------
for i=1:N
    Ti(i) = normrnd(Tin(1),0.1); % Temp air
    Tw(i) = normrnd(Tw_mean,0.1); % Temp wall
    Capw(i) = normrnd(Cw_mean, 50); % Capacitance wall
    Rw(i) = normrnd(Rw_mean,0.001);   % Resistance wall
    Capi(i) = normrnd(Ci_mean,50); % Capacitance air
    Ri(i) = normrnd(Ri_mean,0.001);   % Resistance air
end

% compile ensemble matrix
ensemble_xk = [Ti; Tw; Capw; Rw; Capi; Ri];

%------- Define Function --------
function_f = @ModelEq_v2; % The model equation

function_h = @MeasureEq_v2; % The measure equation

param_h = 0;

for i = 1:length(Tamb)-1;
param = [Tamb(i); Qt(i); Qsol(i)];
```

```
% — Assign Errors —
qk1 = normrnd(0, 0.1^2,[1,N]); % Error Ti 0.01
qk2 = normrnd(0, 1^2,[1,N]); % Error Tw 0.01
qk3 = normrnd(0, 0.001^2,[1,N]); % Error Cap Wall
qk4 = normrnd(0, 0.001^2,[1,N]); % Error Res Wall
qk5 = normrnd(0, 0.001^2,[1,N]); % Error Cap air
qk6 = normrnd(0, 0.0001^2,[1,N]); % Error Res air

% Define error matrix
ensemble_qk = [qk1; qk2; qk3; qk4; qk5; qk6];

% — EnKF Prediction Step —
[ensemble_xk, mean_xkp1, covariance_xkp1] = EnKF_predict(...
    ensemble_xk, ensemble_qk, function_f, param );

% Assign measuremnent error to data point
observation = Tin(i+1) + normrnd(0, gamma^2);

ensemble_epsk = normrnd(0, gamma^2,[1,N]);

% — EnKF Update Step using observation —
[ensemble_xk, mean_xk_a, covariance_xk_a] = EnKF_update(...
    ensemble_xk, ensemble_epsk, function_h, observation, param_h );

% Remove Mean value for value progression
TempCapture_i(i) = mean_xk_a(1);
TempCapture_w(i) = mean_xk_a(2);
CapCapture_w(i) = mean_xk_a(3);
RCapture_w(i) = mean_xk_a(4);
CapCapture_i(i) = mean_xk_a(5);
RCapture_i(i) = mean_xk_a(6);
```

```
end

%%====================== Results Summary ========================

% - Print Out Final Values -
CapForward_w
RForward_w
CapForward_i
RForward_i

Cap_w_std
R_w_std
Cap_i_std
R_i_std

%%------- End of Script -------%%
```

B.1.2 EnKF Prediction Step

```
function [ensemble_xkp1, mean_xkp1, covariance_xkp1] = EnKF_predict(...
    ensemble_xk, ensemble_qk, function_f, param )
%EnKF_predict  Ensemble Kalman Filter predict step
%
% Syntax:
%   [ensemble_xkp1, mean_xkp1, covariance_xkp1] = EnKF_predict(...
%        ensemble_xk, ensemble_qk, function_f, param )
%
% INPUTS:
%   ensemble_xk - M x N ensemble of xk
```

```
%   ensemble_qk – M x N process noise
%   function_f  – Model function that relates xk+1 to xk
%   param   – Parameters of function_f. Default empty
%
% OUTPUTS:
%   ensemble_xkp1   – Forecasted ensemble xk+1
%   mean_xkp1       – Forecasted mean of xk+1
%   covariance_xkp1 – Forecasted covariance of xk+1
%
% Description:
%   Perform Ensemble Kalman Filter prediction step.
%
% Author: Philippe Bisaillon 2012

% Adapted with permission by: Brent Huchuk Dec 2014

%Check input arguments
if nargin < 3
    error('myApp:argChk', 'Not enough input arguments')
end

if nargin < 4
    param = [];
end

if ~strcmp(class( function_f ),'function_handle')
    error('myApp:argChk', 'function_f must be defined a function handle')
end

if nargout > 3
    error('myApp:argChk', 'Too many output arguments')
```

```
end



%Get the dimensions of the ensemble. N is the number of samples and M
%is the dimension of each sample
[M N] = size(ensemble_xk);

if [M N] ~= size( ensemble_qk )
    error('myApp:argChk', ...
        'Dimensions of ensemble and noise matrix are not the same')
end

%forecast each sample
ensemble_xkp1 = zeros(M, N);

for i=1:N
    ensemble_xkp1(:,i) = function_f( ensemble_xk(:,i) , ensemble_qk(:,i) ,...
        param );
end

%the mean is required
if nargout > 1
    mean_xkp1 = mean( ensemble_xkp1 , 2); %get the mean of each row
end

%the covariance is required
if nargout > 2
    ensemble_xkp1_prime = ensemble_xkp1 - repmat(mean_xkp1, 1, N);
    covariance_xkp1 = ensemble_xkp1_prime * ensemble_xkp1_prime' / (N-1);
end
```

B.1.3 EnKF Model Equation

```
function [X] = ModelEq_v2(xk, qk, param);
%%=========================================================================

%desgined to run with Ensemble Kalman Filter

% Dec 7/2013
% Written By: Brent Huhcuk

% v2.0 -  Runs second order model equations for EnKF

%------------------------------ Model Equation ----------------------------------

%------- Initialize parameters --------
dt=30*60;
n = length(xk);

QsolFrac = 0.3;
QtFrac = 0.7;

%===== Param are values for weather =====
Tamb = param(1);
Qt = param(2);
Qsol = param(3);

%==== Assign Errors received from passed vector ====
qk1 = qk(1);
qk2 =qk(2);
```

```
qk3 =qk(3);
qk4 = qk(4);
qk5 = qk(5);
qk6 = qk(6);

%==== Assign Initial value =====

X1_k = xk(1,:);
X2_k = xk(2,:);
X3_k = xk(3,:);
X4_k = xk(4,:);
X5_k = xk(5,:);
X6_k = xk(6,:);

% Predict the values for all states and parameters
for i = 1:1
    % Ti
    X1(i) = dt/X5_k(i)*((X2_k(i) - X1_k(i))/X6_k(i) + Qt*QtFrac +...
        Qsol*(1-QsolFrac)) + X1_k(i) +  sqrt(dt)*qk1*randn();
    %Tw
    X2(i) = dt/X3_k(i)*((Tamb - X2_k(i))/X4_k(i) + (X1_k(i) - ...
        X2_k(i))/X6_k(i) + Qsol*QsolFrac +Qt*(1-QtFrac)) + X2_k(i)...
        +  sqrt(dt)*qk2*randn();

    %CapW
    X3(i) = X3_k(i) + sqrt(dt)*qk3*randn();
    %Rw
    X4(i) = X4_k(i) + sqrt(dt)*qk4*randn();
    %Capi
    X5(i) = X5_k(i) + sqrt(dt)*qk5*randn();
    %Ri
```

```
    X6(i) = X6_k(i) + sqrt(dt)*qk6*randn();
end

% Define predicted values in matrix for reporting back to main script
X = [X1; X2; X3; X4; X5; X6];
end
```

B.1.4 EnKF Update Step

```
function [ensemble_xk_a, mean_xk_a, covariance_xk_a] = EnKF_update(...
    ensemble_xk, ensemble_epsk, function_h, observation, param_h )
%EnKF_update  Ensemble Kalman Filter update step
%
% Syntax:
%   [ensemble_xk_a, mean_xk_a, covariance_xk_a] = EnKF_update( ...
%    ensemble_xk, ensemble_epsk, function_h, ensemble_d, param_h )
%
% INPUTS:
%   ensemble_xk     - M x N ensemble of xk
%   ensemble_epsk   - O x N measurement noise (O depends on the measurement
%                     function)
%   function_h      - Measurement function that relates the measurement to
%                     xk
%   observation         - O x 1 Measurement
%   param_h         - Parameters of function_h. Default empty
%
% OUTPUTS:
%   ensemble_xk_a   - Updated ensemble of xk with new observation
%   mean_xk_a       - Updated mean
%   covariance_xk_a - Updated covariance
```

```
%
% Description:
%   Perform Ensemble Kalman Filter update step.
%
% Author: Philippe Bisaillon 2012

 %Adapted with permission by: Brent Huchuk Dec 2014

%Check input arguments
if nargin < 4
    error('myApp:argChk', 'Not enough input arguments')
end

if nargin < 5
    param_h = [];
end

if ~strcmp(class( function_h ),'function_handle')
    error('myApp:argChk', 'function_h must be defined a function handle')
end

if nargout > 3
    error('myApp:argChk', 'Too many output arguments')
end

%Get the dimensions of the ensemble. N is the number of samples and M is
%the dimension of each sample
[M N] = size(ensemble_xk);

if N ~= length( ensemble_epsk )
    error('myApp:argChk',...
```

```
        'Length of ensemble and noise matrix are not the same')
end

%Create the observation error matrix
O = length(observation);
t_obs = zeros(O, N);
D = zeros(O,N);
In = zeros(N,N);
for i=1:N
    t_obs(i) = function_h( ensemble_xk(:,i) , ensemble_epsk(:,i), param_h);
    D(:,i) = observation - t_obs(:,i);
end

In(:,:) = 1/N;

ensemble_bar = ensemble_xk * In;
ensemble_prime = ensemble_xk - ensemble_bar;
t_obs_prime = t_obs * ( eye(N) - In );

S = t_obs_prime * t_obs_prime' / (N-1);
C = ensemble_prime * t_obs_prime'/ (N-1);

K = C / S;  %Kalman Gain

ensemble_xk_a = ensemble_xk + K * D;

%the mean is required
if nargout > 1
    mean_xk_a = mean( ensemble_xk_a , 2);
end
```

```
%the covariance is required
if nargout > 2
    ensemble_xk_a_prime = ensemble_xk_a - ensemble_xk_a * In;
    covariance_xk_a = ensemble_xk_a_prime * ensemble_xk_a_prime' / (N-1);
end
```

B.1.5 EnKF Measurement Equation

```
function [ tobs ] = MeasureEq_v2( ensemble_xk , ensemble_epsk, param_h )
%%=========================================================================

%desgined to run with Ensemble Kalman Filter

% Dec 7/2013
% Written By: Brent Huhcuk

% v2.0 -  Runs second order model equations for EnKF
%      -  The measurement equation (H) for the EnKF

%------------------------------ Measure Equation ---------------------------------

Hk = [1 0 0 0 0 0];

tobs = Hk*ensemble_xk;

end
```

B.2 Global Optimization

The code contained in this section is an example of the global optimization technique used for the training of the first-order model.

B.2.1 Initialization Program

```
clc
close all
clear all
%%------ Start Here ------%%

% Feb 26/2014
% Written By: Brent Huhcuk

% v1.0 - desgined to use Least Squares in hopes of finding the optimal
%      solution of the 1R1C model



global C1Data ModParT

%%====================== Retrieve Data ========================
load C1Data.txt
%%============================  Global Opt  ==============================

% Define datat arrays
xdata = [Tamb,Tin,Qt];
ydata = Tin;
```

```
% Define first order equation (PDE format)
fun = @(p,xdata) dt/p(2)*(xdata(3) + (xdata(1) - xdata(2))/p(1)) + xdata(2);


% Initial guess for parameter estimates
ModParT(1)=10;   % Resistance
ModParT(2)=1e5;   % Capacitance

% Pass functions to fminsearch funtion
estT = fminsearch('SsqFunT',ModParT);

%%====================== Results Summary ========================

% - Print Out Final Values -
disp('The minimizing values are:');
print('Cap = ');
(estT(2))
print('Res = ');
(estT(1))
%%------- End of Script -------%%
```

B.2.2 Model Equation

```
function xdot=modeleqT(t,x)
%%=============================================================================

%desgined to run with Ensemble Kalman Filter
```

```
% Feb 26/2014
% Written By: Brent Huhcuk

% v1.0 -  Model differential Equation Temperature for 1R1C Global Opt

%------------------------------ Model Equation ----------------------------------
global C1Data ModParT

%------- Initialize parameters --------
nClData=size(C1Data);
nt=nClData(1);           % Number of time steps
dt=60*30;                 % timestep [s]
tu=0:dt:(nt-1)*dt;

% Retrive parameters
GT=ModParT(1);   % Resistance
CT=ModParT(2);   % Capacitance

% Extrapolate for continous data
Tet=interp1(tu,C1Data(:,1),t);
Irradt=interp1(tu,C1Data(:,3),t);

% Predict temp response
xdot(1)=(1/CT )* (  (1/GT)*(Tet -(x(1))) + Irradt  );

%%------- End of Fucntion -------%%
```

B.2.3 Error Equation

```
function q=ssqfunT(p)
%%=========================================================================

%desgined to run with Ensemble Kalman Filter

% Feb 26/2014
% Written By: Brent Huhcuk

% v1.0 -  Model differential Equation Temperature for 1R1C Global Opt

%------------------------------ Sum of Square function ---------------------------
global C1Data ModParT

%------- Initialize parameters --------
nClData=size(C1Data);
nt=nClData(1);          % Number vof time steps
dt=60*5;                % timestep [s]
tu=0:dt:(nt-1)*dt;

% Retrive parameters
ModParT(1)=p(1);   % Resistance
ModParT(2)=p(2);   % Capacitance



Te = C1Data(:,1);   % Exterior Temp
Irra = C1Data(:,3); % Q data
Ti = C1Data(:,2); % Indoor Temp

x0=[Ti(1)];
[t,x]=ode23('ModelEqT',tu,x0);
```

```
% Extrapolate for continous data
Tisim=interp1(t,x(:,1),tu');

% Calculate Sum of Square
uT=(Tisim-Ti);
u=[uT];
q=sum(sum(u.^2));

%%====================== Results Summary ========================
figure(1)

plot(tu,Ti,'b',tu,Tisim,'r')
ylabel('Ti')
legend('meas','sim')

title(['p1-3= ', num2str(p(1)),' ',num2str(p(2)),' NA'])
drawnow
%%------ End of Fucntion ------%%
```

Appendix C

GCL+ Control Code

The code contained in this section is an example of the code used for the actuation of the blinds within the Delta Controls Lab.

```
//==== Predictive Blind Automation Algorithm ====

// - Operating Instructions -
//Blind Automation Algorithm Program
//Turn off HVAC for Experiment by Turning OFF BO2
//Begin Experiment by commanding either BO9 or BO10 to On
//Calculate Solar Irradiance based on Lux reading
//Add digital inputs Light_Override and Blind_Override

// - Define Constants and Variables -

Variable Q_sol //Solar Heat Gain(W)
Variable E_ill //Room Illuminance (Lux)
Variable T_out //Outdoor Air Temp (degC)
Variable T_in //Indoor Air Temp (degC)
Variable CO_2 //CO2 Concentration
Variable Occ_Sensor //Occupancy sensor status
```

```
Variable Occ //State of presence in room
Variable V_State //Visual Comfort State
Variable T_State //Thermal Comfort State
Variable T_Detect //Thermal Comfort Checking
Variable Light_Override // Occupant Control Variable (lights)
Variable Blind_Override // Occupant Control Variable (blinds)
Variable LightSwitch // Value Holding variable
Variable BlindSwitch // Value holding variable
Variable LightState // Value holding variable
Variable BlindState // Value holding variable

Variable d_U // Valuce of Delta U for control decision
Variable T_1 // Predicited temperature timestep 1
Variable T_2 // Predicited temperature timestep 2
Variable T_3 // Predicited temperature timestep 3
Variable T_4 // Predicited temperature timestep 4
Variable T_5 // Predicited temperature timestep 5
Variable T_6 // Predicited temperature timestep 6

Variable U_1 // Predicited U-value timestep 1
Variable U_2 // Predicited U-value timestep 2
Variable U_3 // Predicited U-value timestep 3
Variable U_4 // Predicited U-value timestep 4
Variable U_5 // Predicited U-value timestep 5
Variable U_6 // Predicited U-value timestep 6

Constant A1 = 0.5372 // U-value weighting timestep 1
Constant A2 = 0.1435 // U-value weighting timestep 2
Constant A3 = 0.0383 // U-value weighting timestep 3
Constant A4 = 0.0102 // U-value weighting timestep 4
Constant A5 = 0.0027 // U-value weighting timestep 5
```

```
Constant A6 = 0.007 // U—value weighting timestep 6

Constant CSP = 25 // Cooling Setpoint (degree C)
Constant HSP = 20 // Heating Setpoint (degree C)
Constant R = 0.05 // Thermal resistance (K/W)
Constant C = 2160000 // Thermal Capacitance (J/K)
Constant Tau = 108000 // R*C (S)
Constant d_T = 600 // Delta t for DE assessment (Seconds)

//Assign Occupency and CO2 Sensors
CO_2 = 'AI101 CO2'
Occ_Sensor = 'BI105 MOTION DETECTER'

//— Detections —
//Determine if occupant is in the room (based on occ or CO2)
// keep occupation as on for 60 minutes
If Occ_Sensor = 1 Or CO_2 > 450 Then
Occ = 1
End If
If Occ OnFor 60M Then
Occ = 0
End If

//Determine if occupant has overridden lights
If BI6—Light_Override=1 Then
LightSwitch=1
LightState= CS_RM7206_BLINDS_LIGHT
End If

//Determine if occupant has overridden blinds
If BI7—Blind_Override=1 Then
```

```
BlindSwitch=1
BlindState= 'Blind Control'
End If

//If overrides on either has occured hold override on for 60 minutes
If LightSwitch=1 OnFor 60M
LightSwitch=0
ElseIf LightSwitch=1 And Light_Override—BI6=1 Then
LightSwitch=0
End If

If BlindSwitch=1 OnFor 60M
BlindSwitch=0
ElseIf BlindSwitch=1 And Blind_Override—BI7=1 Then
BlindSwitch=0
End If

Light_Override = BI6
Blind_Override = BI7

//Determine if the lighting level in the room is dark, acceptable or bright
If E_ill < 3 Then
V_State = 0 //Dark
ElseIf E_ill < 20 Then
V_State = 1 //Useful Daylight
Else
V_State = 2 //Bright
End If

//Determine if the lights should be on or off based on override request and
//current conditions.
```

```
If LightSwitch=1 and LightState=OFF Then
V_State = 0 //Dark
ElseIf LightSwitch=1 and LightState=ON Then
V_State = 1 // Useful Daylight
End If

//Determine if the blinds should be up or down based on override request
//and current conditions.
If BlindSwitch=1 and BlindState=Up Then
V_State = 2 //Bright
ElseIf BlindSwitch=1 and BlindState=Down Then
V_State = 1 // Useful Daylight
End If

//Pull in the current temperatures
T_out = CN_RM7206_OAT
T_in = 'AI101 TEMP'

// Correlate illuminance values to solar radiation flux
E_ill = (CN_RM7206_LUXS1 + CN_RM7206_LUXS2) / 2
Q_sol = 12 * E_ill

//Thermal response predictions
DoEvery 10M
T_1 = T_in + ((((T_out - T_in) / R) + Q_sol) * (d_T / C))
T_2 = T_1 + ((((T_out - T_1) / R) + Q_sol) * (d_T / C))
T_3 = T_2 + ((((T_out - T_2) / R) + Q_sol) * (d_T / C))
T_4 = T_3 + ((((T_out - T_3) / R) + Q_sol) * (d_T / C))
T_5 = T_4 + ((((T_out - T_4) / R) + Q_sol) * (d_T / C))
T_6 = T_5 + ((((T_out - T_5) / R) + Q_sol) * (d_T / C))
```

```
//Determine if the temperature predictions fall between setpoints and
//assign the values to the U—values
If T_1 > CSP Then
U_1 = T_1 — CSP
ElseIf T_1 < HSP Then
U_1 = T_1 — HSP
Else
U_1 = 0
End If

If T_2 > CSP Then
U_2 = T_2 — CSP
ElseIf T_2 < HSP Then
U_2 = T_2 — HSP
Else
U_2 = 0
End If

If T_3 > CSP Then
U_3 = T_3 — CSP
ElseIf T_3 < HSP Then
U_3 = T_3 — HSP
Else
U_3 = 0
End If

If T_4 > CSP Then
U_4 = T_4 — CSP
ElseIf T_4 < HSP Then
U_4 = T_4 — HSP
```

```
Else
U_4 = 0
End If

If T_5 > CSP Then
U_5 = T_5 - CSP
ElseIf T_5 < HSP Then
U_5 = T_5 - HSP
Else
U_5 = 0
End If

If T_6 > CSP Then
U_6 = T_6 - CSP
ElseIf T_6 < HSP Then
U_6 = T_6 - HSP
Else
U_6 = 0
End If

d_U = (A1 * U_1) + (A2 * U_2) + (A3 * U_3) + (A4 * U_4) + (A5 * U_5) + (A6 * U_6)
End Do

//Control Decisions based on thermal predictoins
DoEvery 10M
If Q_sol > 0 Then //Check for Daytime

//If system predicts underheating determine wheather to open shades or
//initiate increased flow in the radiant panels.
If d_U < 0 And 'Blind Control' = Down Then
'Blind Control' = Up
```

```
'Cooling Activate' = Off
Else
If d_U < 0 And 'Blind Control' = Up Then
421844.CS_03VVRRP7206 = 100
'Blind Control' = Up
'Cooling Activate' = Off
End If
End If

// — Occupied Periods —
//If system predicts overheating determine wheather to close shades or
//initiate increased ventilation and cooling.
If d_U > 0 And 'Blind Control' = Up Then
'Blind Control' = Down
421844.CS_03VVRRP7206 = 0
'Cooling Activate' = Off
Else
If d_U > 0 And 'Blind Control' = Down Then
'Blind Control' = Down
421844.CS_03VVRRP7206 = 0
'Cooling Activate' = On
End If
End If

//If system remains in temperature range no system should come on
If d_U = 0 Then
'Cooling Activate' = Off
421844.CS_03VVRRP7206 = 0
End If

Else
```

```
// — Unoccupied Periods —

//If system predicts underheating determine wheather to open shades or
//initiate increased flow in the radiant panels.

If d_U < 0 And 'Blind Control' = Up Then
'Blind Control' = Down
Else
If d_U < 0 And 'Blind Control' = Down Then
421844.CS_03VVRRP7206 = 100
'Blind Control' = Down
'Cooling Activate' = Off
End If
End If

//If system predicts overheating determine wheather to close shades or
//initiate increased ventilation and cooling.
If d_U > 0 And 'Blind Control' = Down Then
'Blind Control' = Up
Else
If d_U > 0 And 'Blind Control' = Up Then
'Blind Control' = Up
421844.CS_03VVRRP7206 = 0
'Cooling Activate' = On
End If
End If

//If system remains in temperature range no system should come on
If d_U = 0 Then
'Cooling Activate' = Off
421844.CS_03VVRRP7206 = 0
```

```
End If


End If
// — Visual Comfort Considerations—
// If occupied visual conditions should override the energy decision
If Occ = 1 Then
If V_State < 2 And 'Blind Control' = Down Then
'Blind Control' = Up
ElseIf V_State = 2 And 'Blind Control' = Up Then
'Blind Control' = Down
ElseIf V_State = 0 Then
CS_RM7206_BLINDS_LIGHT = On
End If
End If

//If unoccupied or visually neutral the shades should be open
If V_State > 0 Or Occ = 0 Then
CS_RM7206_BLINDS_LIGHT = Off
End If

End Do
//Report d_U variable for logging purposes
'Heat Balance Variable' = d_U
```